Syntheses, Characterization, and Structural and Kinetic Studies of Half-Open Chromocenes and Their Ligand Adducts

Jeffrey W. Freeman,[†] Noel C. Hallinan,[‡] Atta M. Arif,[†] Robert W. Gedridge,[†] Richard D. Ernst,*[,†] and Fred Basolo*[,‡]

Contribution from the Departments of Chemistry, University of Utah, Salt Lake City, Utah 84112, and Northwestern University, Evanston, Illinois 60208.
Received November 26, 1990. Revised Manuscript Received April 9, 1991

Abstract: The syntheses of a variety of half-open chromocenes from a chromium(II) chloride complex are reported. These complexes may contain either the C_5H_5 or the C_5Me_5 ligand, as well as a variety of pentadienyl ligands (C_5H_7, 3-C_6H_9, 2,3-C_7H_{11}, 2,4-C_7H_{11}, 1,5-$(C_6H_5)_2C_5H_5$, and 1,5-$(Me_3Si)_2C_5H_5$ for C_6H_9 = methylpentadienyl and C_7H_{11} = dimethylpentadienyl). A structural study of Cp*(C_5H_7)Cr was undertaken, revealing much shorter Cr–C(pentadienyl) than Cr–C(Cp*) bonds. The space group is $P2_1/n$ (No. 14) with a = 7.593 (3) Å, b = 23.073 (7) Å, c = 8.530 (4) Å, β = 113.76 (2)°, and V = 1367.7 Å^3, for Z = 4. These 16-electron complexes react with various 2-electron donor ligands (e.g., CO, PF_3, RNC, and $PMe_2C_6H_5$) to yield 18-electron adducts. These species are unusual in that they all contain η^5-S-pentadienyl (S = sickle) ligands. This has been confirmed by a single-crystal X-ray diffraction study of Cp(C_5H_7)Cr(2,6-xylyl isocyanide). The space group is $P2_1/n$ (No. 14), with a = 10.379 (2) Å, b = 7.629 (2) Å, c = 19.961 (4) Å, β = 93.88 (2)°, V = 1576.9 Å^3, and Z = 4. Additionally, a number of 18-electron bisadducts have been prepared in which a η^3-pentadienyl coordination is present. This mode of coordination has been confirmed by an X-ray structural determination of Cp(η^3-C_5H_7)Cr(CO)$_2$, which crystallizes in space group $Pna2_1$ (No. 33), with a = 19.653 (6) Å, b = 6.545 (2) Å, c = 17.126 (5) Å, V = 2202.9 Å^3, and Z = 8. The η^3-C_5H_7 ligands were found to adopt the W configuration. Oxidation of the 18-electron monoadducts by NO^+ to 17-electron monocations regenerates the η^5-U-pentadienyl coordination, revealing that the sickle coordination has only a very small window for stability. Kinetic studies of the CO exchange reactions for the monocarbonyls have been carried out. The exchanges take place by a first-order (dissociative) pathway, with the rates being reasonably comparable to those of their vanadium analogues. Unusually low (even negative) values for ΔS^* have been observed and may be attributed to an η^5-S → η^5-U conversion of the pentadienyl ligands.

Introduction

While the metallocenes have attracted intense interest since their discovery in 1951, their pentadienyl analogues (open metallocenes) have only more recently attracted attention.[1] In a number of chemical, spectroscopic, and structural studies, however, it has already become clear that the open (and half-open) metallocenes differ dramatically from their fully cyclic analogues. Thus, the open metallocenes exhibit rich conformational behavior, much greater degrees of metal–ligand orbital mixing, and much higher degrees of chemical reactivity even though the metal–ligand bonding may be stronger than in the metallocenes.[2] However, for the bis(dienyl)chromium complexes, to date similarities between the two series seem to dominate.[3] Although open chromocenes seem more reactive than chromocene in "naked metal" reactions, neither displays much tendency toward adduct formation (chromocene forms an extremely weakly bound carbonyl, while open chromocenes yield no such species). The compounds are also remarkably similar in a structural sense, with average Cr–C bond distances of 2.169 (4) vs 2.163 (3) Å, respectively, for chromocene and (2,4-C_7H_{11})$_2$Cr (C_7H_{11} = dimethylpentadienyl).

Given these observations, one might not expect to see any real differences for half-open chromocenes such as Cp(C_5H_7)Cr. Notably, however, the half-open chromocenes do exhibit dramatically different behavior than either chromocene or the open chromocenes. For example, the half-open chromocenes form reasonably strongly bound monocarbonyl adducts (vide infra) possessing unusual η^5-S-pentadienyl (S = sickle) coordination and have therefore presented an opportunity to examine the kinetics and mechanism of their CO exchange reactions and to compare these results with those obtained from the open, half-open, and closed vanadium counterparts.[4] Interestingly, the CO exchange reactions have been found to proceed via dissociative pathways, accompanied however by unusually small, even negative, entropies of activation, which appear keenly related to structural natures of the species involved in the exchange process. Herein we present our observations and conclusions regarding the chemistry of the half-open chromocenes.

[†] University of Utah.
[‡] Northwestern University.

Experimental Section

General Procedures. The half-open chromocenes are very air-sensitive and sometimes pyrophoric. Their ligand adducts are slightly to somewhat air-sensitive. All compounds were therefore prepared, handled, and stored under nitrogen and/or in a glovebox, while solutions were generally manipulated on a high vacuum or Schlenk line under N_2, Ar, or CO. Hydrocarbon and ethereal solvents were predried and distilled under N_2 from Na/benzophenone prior to use. Magnetic and spectroscopic data were obtained as described previously.[5] IR and mass spectral data have been included as supplementary material. Elemental analyses were obtained from Desert Analytics (Tucson) and the Analytische Laboratorien (Gummersbach).

The various dienes, phosphines, and phosphites were either purchased or prepared by published procedures.[6] Manipulations of $CrCl_3(THF)_3$[7]

(1) (a) Ernst, R. D. *Chem. Rev.* **1988**, *88*, 1255. (b) Powell, P. In *Advances in Organometallic Chemistry*; West, R., Stone, F. G. A., Eds.; Academic: New York, 1986; Vol. 26, p 125. (c) Kreiter, C. G. *Ibid.* p 297. (d) Yasuda, H.; Nakamura, A. *J. Organomet. Chem.* **1985**, *285*, 15. (e) Bleeke, J. R.; Wittenbrink, R. J.; Clayton, T. W., Jr.; Chiang, M. Y. *J. Am. Chem. Soc.* **1990**, *112*, 6539.

(2) (a) Böhm, M. C.; Eckert-Maksic, M.; Ernst, R. D.; Wilson, D. R.; Gleiter, R. *J. Am. Chem. Soc.* **1982**, *104*, 2699. (b) Kralik, M. S.; Hutchinson, J. P.; Ernst, R. D. *J. Am. Chem. Soc.* **1985**, *107*, 8296. (c) Kralik, M. S.; Rheingold, A. L.; Ernst, R. D. *Organometallics* **1987**, *6*, 2612. (d) Severson, S. J.; Cymbaluk, T. H.; Ernst, R. D.; Higashi, J. M.; Parry, R. W. *Inorg. Chem.* **1983**, *22*, 3833. (e) Bleeke, J. R.; Peng, W.-J. *Organometallics* **1987**, *6*, 1576.

(3) (a) Wilson, D. R.; Liu, J.-Z.; Ernst, R. D. *J. Am. Chem. Soc.* **1982**, *104*, 1120. (b) Newbound, T. D.; Freeman, J. W.; Wilson, D. R.; Kralik, M. S.; Patton, A. T.; Campana, C. F.; Ernst, R. D. *Organometallics* **1987**, *6*, 2432.

(4) (a) Kowaleski, R. M.; Basolo, F.; Trogler, W. C.; Gedridge, R. W.; Newbound, T. D.; Ernst, R. D. *J. Am. Chem. Soc.* **1987**, *109*, 4860. (b) Hallinan, N. C.; Morelli, G.; Basolo, F. *J. Am. Chem. Soc.* **1988**, *110*, 6585. (c) Cheong, M.; Basolo, F. *Organometallics* **1988**, *7*, 2041.

(5) (a) Newbound, T. D.; Stahl, L.; Ziegler, M. L.; Ernst, R. D. *Organometallics* **1990**, *9*, 2962. (b) Evans, D. F. *J. Chem. Soc.* **1959**, 2003.

(6) (a) Jitkow, O. N.; Bogert, M. T. *J. Am. Chem. Soc.* **1941**, *63*, 1979. (b) Klein, J.; Brenner, S. *Isr. J. Chem.* **1969**, *7*, 735. (c) Jutzi, P.; Kohl, F. X. *Organometallic Syntheses*; King, R. B., Eisch, J. J., Eds.; Academic: New York, 1986; Vol. 3, p 489. (d) Heitsch, C. W.; Verkade, J. G. *Inorg. Chem.* **1962**, *1*, 451. (e) Frajerman, C.; Meunier, B. *Inorg. Synth.* **1983**, *22*, 133.

(7) (a) Collman, J. P.; Kittleman, E. T. *Inorg. Synth.* **1966**, *8*, 150. (b) Vavoulis, A.; Austin, T. E.; Tyree, S. Y. *Inorg. Synth.* **1960**, *6*, 129.

0002-7863/91/1513-6509$02.50/0

and dienyl anions[8] were performed on a Schlenk line under an atmosphere of prepurified nitrogen. Unless otherwise stated, the reactions were carried out in 250-mL three-neck round-bottom flasks equipped with magnetic stirring bars and when necessary either pressure-equalizing dropping funnels or solid-addition funnels. Solvent transfers were carried out by syringe. When refluxing of the mixture was required, a water-cooled reflux condenser with a nitrogen inlet was attached. Filtrations utilized coarse glass frits covered with a small amount of Celite.

(Cyclopentadienyl)(pentadienyl)chromium Compounds (Half-Open Chromocenes). The syntheses of the (cyclopentadienyl)(pentadienyl)-chromium compounds (half-open chromocenes) could be carried out by two different methods. Method A was the most general and convenient route and was used to prepare the compounds $Cp(C_5H_7)Cr$ (**1**), $Cp(3\text{-}C_6H_9)Cr$ (**2**), $Cp(2,3\text{-}C_7H_{11})Cr$ (**3**), $Cp(2,4\text{-}C_7H_{11})Cr$ (**4**), $Cp(1,5\text{-}(SiMe_3)_2C_5H_5)Cr$ (**5**), and $Cp(1,5\text{-}(C_6H_5)_2C_5H_5)Cr$ (**6**). Compounds containing the pentamethylcyclopentadienyl ligand could also be prepared. These compounds include $Cp^*(C_5H_7)Cr$ (**7**), $Cp^*(3\text{-}C_6H_9)Cr$ (**8**), and $Cp^*(2,4\text{-}C_7H_{11})Cr$ (**9**). The half-open chromocene $(1,3\text{-}(SiMe_3)_2C_5H_3)(C_5H_7)Cr$ (**10**) was also prepared by method A. Method B could also be used to prepare compounds **1**, **4** (already described in the literature[9]), and **5** but was less convenient than method A. It appears necessary to prepare the "$CrCl_2$" from $CrCl_3$ and Zn in order to obtain the half-open chromocenes selectively. An attempt to prepare $Cp(2,4\text{-}C_7H_{11})Cr$ (**4**) from commercial $CrCl_2$ resulted in the formation of a mixture of Cp_2Cr, $(2,4\text{-}C_7H_{11})_2Cr$, and **4**.

The half-open chromocenes **2**, **3**, and **10** could not be successfully isolated as solids. However, hydrocarbon solutions of **2**, **3**, or **10** could be used to prepare the corresponding ligand monoadducts, which could be isolated as solid products.

Method A. A mixture of 1.9 g (5.0 mmol) of chromium trichloride tris(tetrahydrofuranate) and 0.18 g (2.7 mmol) of powdered zinc in 25 mL of THF was stirred until all the purple $CrCl_3$ had been reduced to light blue "$CrCl_2$". The resulting slurry of "$CrCl_2$" was cooled to −78 °C, and a solution of 5.0 mmol of the desired cyclopentadienide anion and 5.5 mmol of the desired pentadienide anion in 25 mL of THF was slowly added. The resulting brown-red solution was stirred for 1 h at −78 °C, slowly warmed to room temperature, and then stirred for an additional 1–2 h. The solvent was then removed in vacuo and the residue extracted with 3 × 20 mL of hexane (compound **6**, due to its low solubility, was extracted with toluene instead of hexane). The red extracts were combined, filtered, and concentrated to ca. 5–15 mL. The products were obtained by cooling the filtrate to −80 °C and thereafter isolated as dark red crystals.

Method B. A solution of 1.90 g (5.0 mmol) of $[CpCr(O\text{-}t\text{-}C_4H_9)]_2$[10] or 1.30 g (5.0 mmol) of CpCrCl·THF[11] in 30 mL of THF was cooled to −78 °C. Next, a solution of 11.0 mmol of the desired potassium pentadienide in 40 mL of THF was slowly added. The red-brown solution was stirred at −78 °C for 2 h, slowly warmed to room temperature, and stirred for an additional 1–2 h. The solvent was removed in vacuo, the residue was extracted with 3 × 20 mL of hexane, and the extracts were filtered. The product was obtained by concentrating the red filtrate to ca. 20 mL, cooling to −80 °C, and separating the dark red crystals from the greenish supernatant.

Spectroscopic Data. $Cp(C_5H_7)Cr$ (**1**) was isolated as dark red needles from hexane and purified by sublimation at 60–70 °C. Yield: 54% (0.50 g). Mp: 104–105 °C. Anal. Calcd for $C_{10}H_{12}Cr$: C, 65.21; H, 6.57. Found: C, 64.93; H, 6.79.

$Cp(2,4\text{-}C_7H_{11})Cr$[9] (**4**) was isolated as red needles from hexane (large crystals are dark red) and purified by sublimation at 60–70 °C. Yield: method A, av 51% (0.54 g); method B, av 50%. Mp: 116–118 °C. Magnetic susceptibility: 2.9 μ_B. Anal. Calcd for $C_{12}H_{16}Cr$: C, 67.91; H, 7.60. Found: C, 67.65; H, 7.36.

$Cp(1,5\text{-}(SiMe_3)_2C_5H_5)Cr$ (**5**) was isolated as purple-red crystals from pentane and purified by recrystallization from pentane. Yield: 61%. Mp: 77–78 °C. Magnetic susceptibility: 2.7 μ_B. Anal. Calcd for $C_{16}H_{28}CrSi_2$: C, 58.49; H, 8.59. Found: C, 58.48; H, 8.86.

$Cp(1,5\text{-}(C_6H_5)_2C_5H_5)Cr$ (**6**) was isolated as red crystals from toluene and purified by recrystallization from toluene. Yield: 26%. Mp: 225–229 °C dec.

$Cp^*(C_5H_7)Cr$ (**7**) was isolated as dark red needles from hexane and purified by sublimation at 70–80 °C. Yield: 49%. Mp: 83–85 °C. Anal. Calcd for $C_{15}H_{22}Cr$: C, 70.84; H, 8.72. Found: C, 71.23; H, 8.96.

$Cp^*(3\text{-}C_6H_9)Cr$ (**8**) was isolated and purified similarly. Yield: 46%. Mp: 80–81 °C. Anal. Calcd for $C_{16}H_{24}Cr$: C, 71.61; H, 9.01. Found: C, 71.57; H, 9.06.

$Cp^*(2,4\text{-}C_7H_{11})Cr$ (**9**) was isolated and purified similarly at 70–80 °C. Yield: 54%. Mp: 115–117 °C. Anal. Calcd for $C_{17}H_{26}Cr$: C, 72.31; H, 9.28. Found: C, 72.28; H, 9.36.

Synthetic Procedures and Analytical Data for the Half-Open Chromocene Monoadducts. Carbon Monoxide and PF_3 Monoadducts. Due to the toxicity of CO and PF_3 gases, these reactions were carried out in a hood. A 3.0-mmol sample of the desired half-open chromocene was dissolved in 15 mL of hexane (THF was used for compound **6** due to its low solubility in hexane). Carbon monoxide or PF_3 gas was then bubbled through the solution for ca. 30 s. The less reactive **4** was allowed to sit under a CO atmosphere for 10–15 min to ensure complete conversion to the monocarbonyl **4a**. The formation of the monoadduct is generally accompanied by a change in the color of the solution from dark red to yellow-red or orange. The solution was then filtered, concentrated to ca. 5 mL, and cooled to −80 °C. The product was separated from the supernatant and dried under vacuum for 5 min. The monocarbonyls **1a**, **2a**, and **3a** could be filtered through a small (ca. 1-cm) pad of silica instead of Celite. This aided in the removal of unreacted starting material and generally resulted in cleaner products.

Spectroscopic Data. $Cp(C_5H_7)Cr(CO)$ (**1a**) was isolated from hexane as a yellow microcrystalline solid and purified by recrystallization from hexane. Yield: 67% (0.43 g). Mp: 140–141 °C. FT-IR (hexane): 1919.2 cm^{-1}. Anal. Calcd for $C_{11}H_{12}CrO$: C, 62.26; H, 5.70. Found: C, 62.20; H, 5.90. ^1H NMR (benzene-d_6, ambient): δ 4.42 (ddd, 1 H, H3, J = 5.1, 8.2, 9.7 Hz), 3.98 (s, 5 H, C_5H_5), 3.11 (apparent t, 1 H, H4, J = 5.5 Hz), 2.42 (dd, 1 H, H1, J = 2.3, 7.8 Hz), 2.35 (d, 1 H, H6, J = 5.3 Hz), 1.82 (d, 1 H, H7, J = 10.3 Hz), 1.18 (dt, 1 H, H5, J = 5.5, 10.2 Hz), 0.96 (dd, 1 H, H2, J = 2.1, 9.7 Hz). ^{13}C NMR (benzene-d_6, ambient): δ 253.07 (s, 1 C, CO), 90.89 (d, 1 C, J = 163.3 Hz), 86.06 (d, 5 C, C_5H_5, J = 174.6 Hz), 84.18 (d, 1 C, J = 170.8 Hz), 75.73 (d, 1 C, J = 170.8 Hz), 50.92 (t, 1 C, J = 157.0 Hz), 47.39 (t, 1 C, J = 157.0 Hz).

$Cp(C_5H_7)Cr(PF_3)$ (**1d**) was isolated from hexane as a yellow-orange microcrystalline solid and purified by recrystallization from hexane. Yield: 66%. Mp: 105 °C dec. ^1H NMR (benzene-d_6, ambient): δ 4.44 (br s, 1 H, H3), 3.87 (d, 5 H, C_5H_5, J_{P-H} = 2.4 Hz), 3.13 (br s, 1 H, H4), 2.33 (dd, 1 H, H1, J = 5.1, 8.4 Hz), 1.89 (d, 1 H, H6, J = 6.9 Hz), 1.74 (dd, 1 H, H7, J = 7.8, 9.0 Hz), 1.09 (m, 1 H, H5), 0.68 (dd, 1 H, H2, J = 7.4, 18 Hz). ^{13}C NMR (benzene-d_6, ambient): δ 88.89 (d, 1 C, J = 163 Hz), 84.73 (d, 5 C, C_5H_5, J = 176 Hz), 82.10 (d, 1 C, J = 171 Hz), 75.22 (d, 1 C, J = 172 Hz), 47.67 (td, 1 C, J = 155 Hz, J_{P-C} = 15 Hz), 37.09 (td, 1 C, J = 156 Hz, J_{P-C} = 29 Hz).

$Cp(3\text{-}C_6H_9)(CO)Cr$ (**2a**) was isolated from hexane as an orange-yellow microcrystalline solid and purified by recrystallization from hexane. Yield: 63%. Mp: 110–115 °C. FT-IR (hexane): 1919.7 cm^{-1}. Anal. Calcd for $C_{12}H_{14}CrO$: C, 63.71; H, 6.24. Found: C, 63.58; H, 6.37. ^1H NMR (benzene-d_6, ambient): δ 4.31 (apparent t, 1 H, J = 8.7 Hz), 3.94 (s, 5 H, C_5H_5), 2.34 (m, 3 H), 1.43 (s, 3 H, CH_3), 0.77 (m, 2 H). ^{13}C NMR (benzene-d_6, ambient): δ 254.28 (s, 1 C, CO), 91.60 (s, 1 C), 88.78 (d, 1 C, J = 160.8 Hz), 86.81 (d of qnt, 5 C, C_5H_5, J = 176.1, 13.3 Hz), 82.74 (d, 1 C, J = 170.5 Hz), 48.92 (t, 1 C, J = 165.7 Hz), 44.52 (t, 1 C, J = 158.1 Hz), 18.97 (q, 1 C, CH_3, J = 126.5 Hz).

$Cp(2,3\text{-}C_7H_{11})Cr(CO)$ (**3a**) was isolated from hexane as a yellow microcrystalline solid. Yield: 27%. Mp: 123–126 °C. FT-IR (hexane): 1917.2 cm^{-1}. Anal. Calcd for $C_{13}H_{16}CrO$: C, 64.99; H, 6.71. Found: C, 64.93; H, 6.88. ^1H NMR (benzene-d_6, ambient): *isomer a* δ 3.97 (s, 5 H, C_5H_5, overlap with isomer b), 2.35 (m, 3 H), 1.58 (s, 3 H, CH_3), 1.41 (s, 3 H, CH_3), 0.84 (dd, 1 H, J = 5.3, 10.0 Hz), 0.73 (d, 1 H, J = 2.4 Hz); *isomer b* δ 4.12 (apparent t, 1 H, J = 8.6 Hz), 3.97 (s, 5 H, C_5H_5, overlap with isomer a), 2.25 (dd, 1 H, J = 3.3, 8.4 Hz), 2.17 (s, 1 H), 1.79 (s, 1 H), 1.55 (s, 3 H, CH_3), 1.22 (dd, 1 H, J = 3.4, 9.2 Hz), 1.01 (s, 3 H, CH_3). ^{13}C NMR (benzene-d_6, ambient): δ 255.71 (s, 1 C, CO), 100.04 (s, 1 C), 89.37 (s, 1 C), 87.93 (d of qnt, 5 C, C_5H_5, J = 175.0, 6.5 Hz), 84.86 (d, 1 C, J = 171.0 Hz), 48.77 (t, 1 C, J = 155.5 Hz), 47.63 (t, 1 C, J = 156.8 Hz), 21.40 (q, 1 C, CH_3, J = 125.7 Hz), 15.10 (q, 1 C, CH_3, J = 127.0 Hz).

$Cp(2,4\text{-}C_7H_{11})Cr(CO)$ (**4a**) was isolated from hexane as a yellow microcrystalline solid and purified by recrystallization from hexane. Yield: 74%. Mp: 77–80 °C. FT-IR (hexane): 1913.0 cm^{-1}. Anal. Calcd for $C_{13}H_{16}CrO$: C, 64.99; H, 6.71. Found: C, 64.87; H, 6.72. ^1H NMR (benzene-d_6, ambient): δ 4.06 (s, 5 H, C_5H_5), 2.88 (s, 1 H), 2.23 (s, 1 H), 1.88 (s, 1 H), 1.81 (s, 1 H), 1.52 (s, 3 H, CH_3), 1.41 (s, 1 H), 1.18 (s, 3 H, CH_3). ^{13}C NMR (benzene-d_6, ambient): δ 255.26 (s, 1 C, CO), 105.98 (s, 1 C), 94.28 (s, 1 C), 87.92 (d, 5 C, C_5H_5, J = 172 Hz),

(8) (a) Wilson, D. R.; Stahl, L.; Ernst, R. D. *Organometallic Syntheses*; King, R. B., Eisch, J. J., Eds.; Academic: New York, 1986; Vol. 3, p 136. (b) Yasuda, H.; Nishi, T.; Lee, K.; Nakamura, A. *Organometallics* **1983**, *2*, 21.

(9) Freeman, J. W.; Wilson, D. R.; Ernst, R. D.; Smith, P. D.; Klendworth, D. D.; McDaniel, M. P. *J. Polym. Sci., Part A: Polym. Chem.* **1987**, *25*, 2063.

(10) Chisholm, M. H.; Cotton, F. A.; Extine, M. W.; Rideout, D. C. *Inorg. Chem.* **1979**, *18*, 120.

(11) (a) Moran, H. *Transition Met. Chem. (London)* **1981**, *6*, 173. (b) Fischer, E. O.; Ulm, K.; Kuzel, P. *Z. Anorg. Allg. Chem.* **1963**, *319*, 253.

78.87 (d, 1 C, J = 162 Hz), 46.54 (t, 1 C, J = 157 Hz), 45.96 (t, 1 C, J = 157 Hz), 24.78 (q, 1 C, CH_3, J = 124.5 Hz), 17.57 (q, 1 C, CH_3, J = 124.2 Hz).

Cp(1,5-$(SiMe_3)_2C_5H_5$)Cr(CO) (5a) was isolated from hexane as an orange microcrystalline solid. Yield: 77%. Mp: 59–62 °C. FT-IR (hexane): 1903.7 cm^{-1}. Anal. Calcd for $C_{17}H_{28}CrOSi_2$: C, 57.26; H, 7.91. Found: C, 56.75; H, 8.11. ^1H NMR (benzene-d_6): δ 4.73 (dd, 1 H, H3, J = 5.1 11.7 Hz), 4.13 (s, 5 H, C_5H_5), 3.36 (apparent t, 1 H, H4, J = 5.4 Hz), 1.58 (d, 1 H, H7, J = 12.3 Hz), 1.41 (dd, 1 H, H5, J = 6.2, 12.2 Hz), 0.64 (d, 1 H, H2, J = 12.0 Hz), 0.19 (s, 9 H, $SiMe_3$), 0.08 (s, 9 H, $SiMe_3$). ^{13}C NMR (benzene-d_6, ambient): δ 257.39 (s, 1 C, *C*O), 97.62 (d, 1 C, J = 161.7 Hz), 92.56 (d, 1 C, J = 164.4 Hz), 85.99 (d, 5 C, C_5H_5, J = 174.8 Hz), 77.45 (d, 1 C, J = 164.6 Hz), 60.18 (d, 1 C, J = 138.4 Hz), 56.78 (d, 1 C, J = 136.9 Hz), 0.63 (q, 3 C, $SiMe_3$, J = 118 Hz), 0.50 (q, 3 C, $SiMe_3$, J = 118 Hz).

Cp(1,5-$(C_6H_5)_2C_5H_5$)Cr(CO) (6a) was isolated from THF–hexane as a yellow-orange microcrystalline solid. Yield: 81%. Mp: 200–205 °C dec. FT-IR (hexane): 1912.4 cm^{-1}. Anal. Calcd for $C_{23}H_{20}CrO$: C, 75.81; H, 5.53. Found: C, 75.41; H, 5.63. ^1H NMR (acetone-d_6, ambient): δ 7.15 (m, 5 H, C_6H_5), 7.08 (m, 5 H, C_6H_5), 5.79 (dd, 1 H, H3, J = 5.3, 9.8 Hz), 4.33 (s, 5 H, C_5H_5), 3.80 (apparent t, 1 H, H4, J = 5.7 Hz), 3.40 (d, 1 H, H5, J = 9.9 Hz), 2.78 (d, 1 H, H7, J = 9.3 Hz), 2.41 (dd, 1 H, H2, J = 6.5, 10.3 Hz). ^{13}C NMR (benzene-d_6, ambient): δ 256.52 (s, 1 C, *C*O), 143.50 (s, 1 C), 141.90 (s, 1 C), 137.84 (d, 1 C, J = 158 Hz), 128.72 (dd, 2 C, J = 158.5, 7 Hz), 128.60 (dd, 2 C, J = 158.5, 7 Hz), 126.01 (dd, 2 C, J = 156.6, 8 Hz), 125.79 (dd, 2 C, J = 156.6, 8 Hz), 125.49 (dd, 2 C, J = 156.8, 8 Hz), 91.31 (d, 1 C, J = 163.3 Hz), 89.64 (d of qnt, 5 C, C_5H_5, J = 175.4, 6.5 Hz), 80.23 (d, 1 C, J = 173.3 Hz), 70.70 (d, 1 C, J = 175.3 Hz), 70.57 (d, 1 C, J = 152.3 Hz), 67.36 (d, 1 C, J = 156 Hz).

Cp*(C_5H_7)Cr(CO) (7a) was isolated from hexane as a yellow-orange microcrystalline solid. Yield: 66%. Mp: 139–140 °C. FT-IR (hexane): 1902.8 cm^{-1}. Anal. Calcd for $C_{16}H_{22}CrO$: C, 68.06; H, 7.85. Found: 68.38; H, 8.28. ^1H NMR (benzene-d_6, ambient): δ 3.79 (ddd, 1 H, H3, J = 5.1, 7.8, 9.0 Hz), 2.47 (d, 1 H, H6, J = 5.1 Hz), 2.27 (apparent t, 1 H, H4, J = 5.5 Hz), 1.91 (dd, 1 H, H1, J = 7.8, 3.0 Hz), 1.55 (dt, 1 H, H5, J = 5.7, 9.5 Hz), 1.36 (s, 15 H, C_5Me_5), 1.19 (d, 1 H, H7, J = 9.6 Hz), 1.09 (dd, 1 H, H2, J = 9.5, 2.0 Hz). ^{13}C NMR (benzene-d_6, ambient): δ 254.78 (s, 1 C, *C*O), 97.13 (d, 1 C, J = 160 Hz), 96.66 (s, 5 C, C_5Me_5), 85.63 (d, 1 C, J = 170 Hz), 83.00 (d, 1 C, 170 Hz), 56.75 (t, 1 C, J = 155 Hz), 48.88 (t, 1 C, J = 158 Hz), 10.30 (q, 5 C, C_5Me_5, J = 126 Hz).

Cp*(3-C_6H_9)Cr(CO) (8a) was isolated from hexane as an orange microcrystalline solid. Yield: 73%. Mp: 118–120 °C. FT-IR (hexane): 1900.8 cm^{-1}. Anal. Calcd for $C_{17}H_{24}CrO$: C, 68.90; H, 8.16. Found: C, 68.97; H, 8.37. ^1H NMR (benzene-d_6, ambient): δ 3.67 (apparent t, 1 H, H3, J = 8.4 Hz), 2.25 (d, 1 H, H6, J = 5.1 Hz), 1.82 (dd, 1 H, H1, J = 2.7, 7.5 Hz), 1.63 (d, 1 H, H7, J = 9.3 Hz), 1.46 (s, 3 H, CH_3), 1.41 (s, 15 H, C_5Me_5), 1.14 (dd, 1 H, H5, J = 5.4, 9.6 Hz), 0.96 (dd, 1 H, H2, J = 3.0, 8.7 Hz). ^{13}C NMR (benzene-d_6, ambient): δ 256.03 (s, 1 C, CO), 96.79 (s, 5 C, C_5Me_5) 93.32 (d, 1 C, J = 158.9 Hz), 91.69 (s, 1 C), 81.83 (d, 1 C, J = 169.8 Hz), 53.37 (t, 1 C, J = 155.4 Hz), 47.02 (t, 1 C, J = 153.0 Hz), 15.08 (q, 1 C, CH_3, J = 127.0 Hz), 10.42 (q, 5 C, C_5Me_5, J = 125.7 Hz).

Cp*(2,4-C_7H_{11})Cr(CO) (9a) was isolated similarly. Yield: 78%. Mp: 95–97 °C. Anal. Calcd for $C_{18}H_{26}CrO$: C, 69.65; H, 8.44. Found: C, 69.69; H, 8.58. ^1H NMR (benzene-d_6, ambient): δ 2.30 (s, 1 H), 1.93 (s, 1 H), 1.76 (d, 1 H, J = 3.9 Hz), 1.70 (s, 3 H, CH_3), 1.47 (s, 15 H, C_5Me_5), 1.43 (d, 1 H, J = 4.2 Hz), 1.32 (s, 3 H, CH_3), 1.07 (s, 1 H). ^{13}C NMR (benzene-d_6, ambient): δ 257.18 (s, 1 C, *C*O), 109.93 (s, 1 C), 97.17 (s, 5 C, C_5Me_5), 93.36 (t, 1 C, J = 5 Hz), 82.37 (d, 1 C, J = 157 Hz), 52.52 (td, 1 C, J = 154, 5 Hz), 45.08 (t, 1 C, J = 156 Hz), 21.56 (q, 1 C, CH_3, J = 125 Hz), 18.21 (q, 1 C, CH_3, J = 125 Hz), 10.67 (q, 5 C, C_5Me_5, J = 126 Hz).

(1,3-$(SiMe_3)_2C_5H_3$)(C_5H_7)Cr(CO) (10a) was isolated from hexane as a red-orange microcrystalline solid. Yield: 35%. Mp: 68–69 °C. ^1H NMR (benzene-d_6, ambient): δ 4.73 (m, 1 H, H3), 4.53 (s, 1 H, Cp), 4.26 (s, 1 H, Cp), 4.20 (s, 1 H, Cp), 3.48 (apparent t, 1 H, H4, J = 5.4 Hz), 2.59 (d, 1 H, H1, J = 7.5 Hz), 2.26 (d, 1 H, H6, J = 5.1 Hz), 2.09 (d, 1 H, H7, J = 9.9 Hz), 1.17 (m, 1 H, H5), 1.02 (d, 1 H, H2, J = 9.0 Hz), 0.12 (s, 9 H, $SiMe_3$), 0.08 (s, 9 H, $SiMe_3$).

Isocyanide Adducts. Due to the unstable nature of the mono(*tert*-butyl isocyanide) adducts, the procedure should be carried out quickly in order to minimize the formation of the bis(*tert*-butyl isocyanide) adducts. A 2.5-mmol sample of **1**, **4**, or **7** was dissolved in 15 mL of hexane, and then 2.7 mmol of *tert*-butyl isocyanide was added to the solution by syringe, resulting in an immediate color change from dark red to bright red-orange. The solution was immediately filtered and concentrated to ca. 5 mL. The filtrate was then cooled to −80 °C for 1–2 days. The orange microcrystalline product was isolated by syringing out the supernatant and dried under vacuum. The product is best stored at −30 °C to prevent the formation of the bis(isocyanide) adduct.

Spectroscopic Data. **Cp(C_5H_7)Cr(CN(*t*-C_4H_9)) (1b)** was isolated from hexane as an orange microcrystalline solid that melted to a red-orange oil below room temperature. The oil slowly disproportionated to a mixture of **1** and **1h**, so no elemental analysis was obtained. ^1H NMR (benzene-d_6, ambient): δ 4.65 (br s, 1 H, H3), 4.13 (s, 5 H, C_5H_5), 3.25 (br s, 1 H, H4), 2.43 (d, 1 H, H1, J = 7.5 Hz), 2.23 (d, 1 H, H6, J = 4.5 Hz), 2.10 (d, 1 H, H7, J = 9.3 Hz), 1.03 (s, 9 H, *t*-C_4H_9), 0.85 (d, 1 H, H2, J = 9.3 Hz), 0.80 (overlap with signal at 0.84, 1 H, H5). ^{13}C NMR (benzene-d_6, ambient): δ 218.02 (s, 1 C, *C*NR), 91.05 (d, 1 C, J = 160 Hz), 85.39 (d, 5 C, C_5H_5, J = 174 Hz), 84.14 (d, 1 C, J = 174 Hz), 74.96 (d, 1 C, J = 174 Hz), 57.03 (s, 1 C, $C(CH_3)_3$), 50.68 (t, 1 C, J = 156 Hz), 46.23 (t, 1 C, J = 156 Hz), 31.88 (q, 3 C, $C(CH_3)_3$, J = 127 Hz).

Cp(2,4-C_7H_{11})Cr(CN(*t*-C_4H_9)) (4b) was isolated from hexane as an orange microcrystalline solid (mp 45 °C dec) that slowly disproportionated at room temperature to a mixture of **4** and **4h**. ^1H NMR (benzene-d_6, ambient): δ 4.19 (s, C_5H_5), 2.99 (s, 1 H), 2.16 (s, 1 H), 2.03 (s, 1 H), 1.80 (s, 1 H), 1.75 (s, 3 H, CH_3), 1.35 (s, 1 H), 1.26 (s, 3 H, CH_3), 1.08 (s, 9 H, *t*-C_4H_9). ^{13}C NMR (benzene-d_6, ambient): δ 222.93 (s, 1 C *C*NR), 105.13 (s, 1 C), 90.15 (s, 1 C), 87.63 (d, 5 C, C_5H_5, J = 173.1 Hz), 77.52 (d, 1 C, J = 165.5 Hz), 57.02 (s, 1 C, $C(CH_3)_3$), 45.61 (t, 1 C, J = 153.5 Hz), 45.51 (t, 1 C, J = 153.5 Hz), 32.03 (q, 3 C, $C(CH_3)_3$, J = 127.0 Hz), 25.35 (q, 1 C, J = 126.5 Hz), 17.69 (q, 1 C, J = 125.7 Hz).

Cp*(C_5H_7)Cr(CN(*t*-C_4H_9)) (7b) was isolated from hexane as a red-orange microcrystalline solid (mp 74–45 °C) that was more thermally stable than either **1b** or **4b**. Anal. Calcd for $C_{20}H_{31}CrN$: C, 71.18; H, 9.26. Found: C, 70.82; H, 9.28. ^1H NMR (benzene-d_6, ambient): δ 3.96 (ddd, 1 H, H3, J = 4.8, 7.5, 9.6 Hz), 2.39 (apparent t, 1 H, H4, J = 5.1 Hz), 2.25 (d, 1 H, H6, J = 5.0 Hz), 1.88 (ddd, 1 H, H1, J = 7.5, 2.0, 0.9 Hz), 1.52 (s, 15 H, C_5Me_5), 1.39 (d, 1 H, H7, J = 8.4 Hz), 1.13 (dt, 1 H, H5, J = 5.3, 8.7 Hz), 1.06 (s, 9 H, *t*-C_4H_9), 0.96 (ddd, 1 H, H2, J = 0.9, 1.8, 9.6 Hz). ^{13}C NMR (benzene-d_6, ambient): δ 221.53 (s, 1 C, *C*NR), 97.11 (d, 1 C, J = 158.8 Hz), 95.11 (s, 5 C, C_5Me_5), 85.83 (d, 1 C, J = 171.9 Hz), 82.17 (d, 1 C, J = 167.5 Hz), 56.58 (t, 1 C, J = 154.4 Hz), 56.23 (s, 1 C, $C(CH_3)_3$), 47.90 (t, 1 C, J = 156.6 Hz), 32.04 (q, 3 C, $C(CH_3)_3$, J = 126.7 Hz), 10.70 (q, 5 C, C_5Me_5, J = 126.7 Hz).

For the preparation of Cp(C_5H_7)Cr(CN-2,6-$(CH_3)_2C_6H_3$) (**1c**), 0.30 g (1.6 mmol) of **1** was dissolved in 25 mL of hexane. Next, a solution of 0.20 g (1.7 mmol) of 2,6-xylyl isocyanide dissolved in 10 mL of hexane was added to the solution of **1**. The color of the mixture rapidly turned bright red-orange. The solution was filtered and concentrated to ca. 25 mL, during which time crystals of **1c** began to form. The filtrate was cooled to −20 °C for 1 day. The red-orange crystalline product was then isolated and dried under vacuum. Yield: 0.40 g (78%). Mp: 95–97 °C. Anal. Calcd for $C_{19}H_{21}CrN$: C, 72.36; H, 6.71. Found: C, 72.07; H, 6.77. ^1H NMR (benzene-d_6, ambient): δ 6.75 (s, 3 H, C_6H_3), 4.70 (dt, 1 H, H3, J = 3.9, 8.7 Hz), 4.18 (s, 5 H, C_5H_5), 3.35 (apparent t, 1 H, H4, J = 5.4 Hz), 2.56 (d, 1 H, H1, J = 7.2 Hz), 2.39 (d, 1 H, H6, J = 5.1 Hz), 2.18 (d, 1 H, H7, J = 9.3 Hz), 2.13 (s, 6 H, CH_3), 1.13 (m, 1 H, H5), 1.07 (d, 1 H, H2, J = 9.3 Hz). ^{13}C NMR (benzene-d_6, ambient): δ 220.87 (s, 1 C, *C*NR), 132.30 (s, 1 C), 130.97 (s, 1 C), 127.85 (d, 2 C, J = 156 Hz), 125.01 (d, 2 C, J = 159 Hz), 91.96 (d, 1 C, 160 Hz), 85.95 (d of qnt, 5 C, C_5H_5, J = 173, 7 Hz), 84.67 (d, 1 C, J = 171 Hz), 75.52 (d, 1 C, J = 172 Hz), 51.19 (t, 1 C, J = 155 Hz), 48.27 (t, 5 C, J = 157 Hz), 19.13 (q, 2 C, CH_3, J = 127 Hz).

Phosphine and Phosphite Adducts. A 2.5-mmol sample of P(OCH_2)$_3$$CCH_3$ (caution: toxic) in 5 mL of THF was added to a solution containing ca. 2.3 mmol of **1** or **3** in 15 mL of hexane, resulting in an immediate color change from dark red to orange. The product tended to crystallize out of solution if too much hexane was present. The solvent was removed in vacuo and the residue extracted with 3 × 15 mL of toluene. The extracts were filtered, concentrated to 5–10 mL, and cooled to −30 °C for 1–2 days. The orange crystals that formed were isolated and dried under vacuum.

Spectroscopic Data. **Cp(C_5H_7)Cr(P(OCH_2)$_3$$CCH_3$) (1e)** was isolated as orange crystals. Yield: 83%. Mp: 128–130 °C. Anal. Calcd for $C_{15}H_{21}CrO_3P$: C, 54.22; H, 6.37. Found: C, 54.92; H, 6.75. ^1H NMR (benzene-d_6, ambient): δ 4.69 (m, 1 H, H3), 4.25 (d, 5 H, C_5H_5, J_{P-H} = 2.2 Hz), 3.48 (d, 6 H, P(OCH_2)$_3$$CCH_3$, J_{P-H} = 4.2 Hz), 3.30 (apparent t, 1 H, H4, J = 5.0 Hz), 2.65 (dd, 1 H, H1, J = 5.0, 8.1 Hz), 2.35 (d, 1 H, H6, J = 7.6 Hz), 2.17 (dd, 1 H, H7, J = 7.4, 8.9 Hz), 1.42 (m, 1 H, H5), 1.26 (dd, 1 H, H2, J = 17.9, 8.5 Hz), −0.26 (s, 3 H, P(OCH_2)$_3$$CCH_3$). ^{13}C NMR (benzene-d_6, ambient): δ 88.96 (d, 1 C, J = 160 Hz), 84.65 (d of qnt, 5 C, C_5H_5, J = 175, 6.5 Hz), 81.31 (dt, 1 C, J = 170, 6 Hz), 74.80 (td, 3 C, P(OCH_2)$_3$$CCH_3$, J = 150, J_{P-C} = 7.4 Hz), 74.32 (d, 1 C, J = 170 Hz), 47.73 (td, 1 C, J = 155, J_{P-C} = 13.5

Hz), 39.80 (td, 1 C, J = 156, J_{P-C} = 25.5 Hz), 31.46 (d, 1 C, P(OCH_2)$_3$CCH_3, J_{P-C} = 28.5 Hz), 14.77 (q, 1 C, P(OCH_2)$_3$CCH_3, J = 126 Hz).

Cp(2,3-C_7H_{11})Cr(P(OCH_2)$_3$CCH_3) (3e) was isolated as orange crystals from toluene and purified by recrystallization from toluene. Yield: 33%. Mp: 141–142 °C. Anal. Calcd. for $C_{17}H_{25}CrO_3P$: C, 56.66; H, 6.99. Found: C, 56.20; H, 6.98. ^{1}H NMR (benzene-d_6, ambient): δ 4.23 (s, 5 H, C_5H_5), 3.50 (s, P(OCH_2)$_3$CCH$_3$, 6 H), 2.61 (m, 2 H), 2.18 (s, 1 H), 1.92 (s, 3 H, CH_3), 1.67 (s, 3 H, CH_3), 0.98 (br s, 1 H), 0.92 (s, 1 H), –0.23 (s, 3 H, P(OCH_2)$_3$CCH_3). ^{13}C NMR (benzene-d_6, ambient): δ 97.99 (s, 1 C), 87.19 (s, 1 C), 86.83 (d of qnt, 5 C, C_5H_5, J = 174.4, 6.5 Hz), 83.08 (d, 1 C, J = 170.0 Hz), 74.92 (td, 3 C, P(OCH_2)$_3$CCH$_3$, J = 148.1 J_{P-C} = 7.7 Hz), 45.96 (td, 1 C, J = 154.7, J_{P-C} = 14.3 Hz), 40.66 (td, 1 C, J = 154.7, J_{P-C} = 28.6 Hz), 31.59 (d, 1 C, P(OCH_2)$_3$CCH_3, J_{P-C} = 28.0 Hz), 22.23 (q, 1 C, J = 127.5 Hz), 15.18 (q, 1 C, J = 126.0 Hz), 14.92 (q, 1 C, P(OCH_2)$_3$CCH_3, J = 127.5 Hz).

Cp(C_5H_7)Cr(P(OCH_3)$_3$) (1f). A 0.46-g (2.5-mmol) sample of **1** was dissolved in 15 mL of hexane, and then 0.32 mL (2.7 mmol) of trimethyl phosphite was added to the solution by syringe, resulting in a barely noticeable color change from dark red to a brighter red. The solution was filtered, concentrated to ca. 10 mL, and cooled to –80 °C for 1 day. The bright red needles of **1f** were isolated and dried under vacuum. Yield: 84% (0.65 g). Mp: 53–55 °C. Anal. Calcd for $C_{13}H_{21}CrO_3P$: C, 50.65; H, 6.87. Found: C, 51.39; H, 6.87. ^{1}H NMR (benzene-d_6, ambient): δ 4.75 (br s, 1 H), 4.00 (s, 5 H, C_5H_5), 3.32 (s, 1 H), 3.26 (d, free P(OCH_3)$_3$, J = 10.8 Hz), 3.23 (s, 9 H, bound P(OCH_3)$_3$, J = 11.1 Hz), 2.40 (dd, 1 H, J = 5.4, 8.1 Hz), 2.28 (d, 1 H, J = 6.6 Hz), 2.20 (dd, 1 H, J = 6.9, 9.0 Hz), 1.03 (m, 2 H). ^{13}C NMR (benzene-d_6, ambient): δ 89.55 (d, 1 C, J = 158 Hz), 84.15 (d, 5 C, C_5H_5, J = 173 Hz), 83.52 (d, 1 C, J = 170 Hz), 75.05 (d, 1 C, J = 170 Hz). The J_{C-H} values for the following signals could not be obtained: δ 51.78 (1 C, J_{P-H} = 6.5 Hz), 49.50 (bound P(OCH_3)$_3$, J_{P-H} = 14.5 Hz), 48.96 (free P(OCH_3)$_3$, J_{P-H} = 9.8 Hz), 39.41 (J_{P-H} = 2.45 Hz).

Cp(C_5H_7)Cr(PMe_2Ph) (1g). A 0.46-g (2.5-mmol) sample of **1** was dissolved in 15 mL of hexane, and then 0.38 mL (2.7 mmol) of dimethylphenylphosphine was added to the solution by syringe, resulting in the formation of a small amount of green powder in 10–15 min. The solution was then filtered and cooled to –30 °C. The dark red product was isolated and dried under vacuum. Attempts to recrystallize the product from toluene resulted in the isolation of a mixture of **1** and **1g**. The compounds **1** and **1g** can be differentiated on the basis of their crystal habits; **1g** forms nodules while **1** forms long, needlelike crystals. Yield: 47% (0.38 g). Mp: 65–67 °C. ^{1}H NMR (toluene-d_8, –40 °C): δ 7.30 (s, PMe$_2$P*h*), 4.62 (s, 1 H), 3.77 (s, 5 H, C_5H_5), 3.11 (s, 1 H), 1.95 (s, 2 H), 1.04 (s, P*Me*$_2$Ph), 0.28 (s, 1 H), 0.7 (br s, 2 H). ^{13}C NMR (toluene-d_8, –40 °C): δ 90.68, 85.15, 84.88 (C_5H_5), 75.35, 48.24 (d, J_{P-H} = 7 Hz), 40.19 (d, J_{P-H} = 18 Hz). Most of the PMe$_2$Ph signals were obscured by the solvent.

Bis(ligand) Adducts of the Half-Open Chromocenes. The bis(*tert*-butyl isocyanide) adducts of **1** and **4** could be prepared by two methods. Method A for compound **4h** resulted in the formation of one major isomer while method B resulted in the formation of two isomers in ca. 60:40 ratio. Compound **1h** formed two isomers by both methods.

Method A. Hexane solutions of **1b** and **4b** with 1 equiv of *tert*-butyl isocyanide or solutions of **1** and **4** with 2 equiv of *tert*-butyl isocyanide were allowed to sit at room temperature for 2 weeks. The resulting deep red solutions were then filtered, and the solvent was removed in vacuo, leaving behind dark red oils.

Method B. Hexane solutions of **1b** and **4b** with 1 equiv of *tert*-butyl isocyanide or solutions of **1** and **4** with 2 equiv of *tert*-butyl isocyanide were refluxed for 2–3 h. The deep red solutions were filtered and the solvent removed in vacuo, leaving behind dark red oils.

Spectroscopic Data. Cp(C_5H_7)Cr(CN-*t*-C_4H_9)$_2$ (1h). Compound **1h** was isolated as a deep red oil. ^{1}H NMR (benzene-d_6, ambient): δ 6.58 (br s, 1 H), 6.07 (br s, 1 H), 5.14 (s, 2 H), 4.88 (s, 1 H), 4.78 (s, 1 H), 4.30 (s, 5 H, C_5H_5), 4.23 (s, 5 H, C_5H_5), 3.39 (s, 1 H), 2.84 (s, 1 H), 2.59 (s, 1 H), 1.65 (s, 1 H), 1.48 (s, 1 H), 1.28 (*t*-C_4H_9), 1.21 (*t*-C_4H_9), 1.12 (*t*-C_4H_9), 0.54 (s, 1 H). ^{13}C NMR (benzene-d_6, ambient): δ 231.69 (*C*NR), 227.40 (*C*NR), 224.13 (*C*NR), 217.93 (*C*NR), 147.39, 142.66, 105.27, 104.81, 87.67 (Cp), 87.06 (Cp), 85.75, 76.13, 69.48, 64.48, 57.25 ($C(CH_3)_3$), 56.86 ($C(CH_3)_3$), 56.69 (C, $C(CH_3)_3$), 56.27 ($C(CH_3)_3$), 42.29, 41.48, 32.70 (C(CH_3)$_3$), 32.46 (C(CH_3)$_3$), 31.97 (C(CH_3)$_3$), 31.84 (C(CH_3)$_3$).

Cp(2,4-C_7H_{11})Cr(CN-*t*-C_4H_9)$_2$ (4h). Compound **4h** was isolated as a deep red oil. ^{1}H NMR (benzene-d_6, ambient): δ 5.20 (s, 1 H), 5.09 (s, 1 H), 4.35 (s, 5 H, C_5H_5), 2.63 (s, 1 H), 2.54 (s, 1 H), 2.11 (s, 3 H, CH_3), 1.98 (s, 3 H, CH_3), 1.55 (s, 1 H), 1.14 (s, 9 H, *t*-C_4H_9). ^{13}C NMR (benzene-d_6, ambient): δ 230.70 (s, 1 C, *C*NR), 213.74 (s, 1 C, *C*NR), 149.04 (s, 1 C), 107.92 (t, 1 C, J = 154.5 Hz), 94.55 (s, 1 C), 87.49 (d of qnt, 5 C, C_5H_5, J = 173.7, 6.5 Hz), 61.94 (d, 1 C, J = 149.4 Hz), 56.72 (s, 1 C, $C(CH_3)_3$), 55.68 (s, 1 C, $C(CH_3)_3$), 45.80 (t, 1 C, J = 153.8 Hz), 32.17 (q, 3 C, C(CH_3)$_3$, J = 127.4 Hz), 31.98 (q, 3 C, C(CH_3)$_3$, J = 127.7 Hz), 27.15 (q, 1 C, CH_3, J = 124.6 Hz), 22.78 (q, 1 C, CH_3, J = 125.8 Hz).

Dicarbonyl and Bis(phosphine) Adducts of the Half-Open Chromocenes. Since some of these reactions involved the use of toxic CO gas and high pressures, they were carried out in a hood and behind a blast shield. A 2.5-mmol sample of **1**, **4**, or **7** was dissolved in 30 mL of hexane and syringed into a Fischer–Porter pressure tube under a CO atmosphere. The CO pressure was then increased to ca. 5 atm, and the bottom 10–15 cm of the tube was heated to ca. 70 °C in an oil bath. The pressure tube was heated for 36 h for compounds **1** and **7** while for compound **4** the pressure tube was heated for 6 days. At the end of the reaction period, the oil bath was removed and the excess CO was vented into a hood. The yellow solution was then syringed out and filtered. For compounds **1i** and **7i**, the filtrate was concentrated to ca. 20 mL and then cooled to –30 °C. For compound **4i**, the filtrate was concentrated to ca. 5 mL and cooled to –80 °C.

Spectroscopic Data. Cp(C_5H_7)Cr(CO)$_2$ (1i) was isolated as bright yellow needles from hexane and purified by recrystallization from hexane. Yield: 86% (0.52 g). Mp: 81–82 °C. FT-IR (hexane): 1950.1, 1890.2 cm^{-1}. Anal. Calcd for $C_{12}H_{12}CrO_2$: C, 60.00; H, 5.03. Found: C, 59.83; H, 5.12. ^{1}H NMR (benzene-d_6, ambient): δ 5.57 (dt, 1 H, H5, J = 10.2 16.8 Hz), 5.31 (dd, 1 H, H6, J = 16.8, 1.5 Hz), 4.83 (dd, 1 H, H7, J = 10.2, 1.5 Hz), 4.01 (s, 5 H, C_5H_5), 3.81 (dt, 1 H, H3, J = 6.9, 10.2 Hz), 2.53 (dd, 1 H, H1, J = 6.9, 1.8 Hz), 1.61 (apparent t, 1 H, H4, J = 10.5 Hz), 0.52 (dd, 1 H, H2, J = 10.5, 1.8 Hz). ^{13}C NMR (benzene-d_6, ambient): δ 249.51 (s, 1 C, CO), 247.38 (s, 1 C, CO), 138.54 (d, 1 C, J = 149 Hz), 112.77 (t, 1 C, J = 157 Hz), 88.24 (d of qnt, 5 C, C_5H_5, J = 176, 7 Hz), 73.08 (d, 1 C, J = 162 Hz), 72.11 (d, 1 C, J = 155 Hz), 42.67 (t, 1 C, J = 161 Hz).

Cp(2,4-C_7H_{11})Cr(CO)$_2$ (4i) was isolated from hexane as a bright yellow solid that melted below room temperature. FT-IR (hexane): 1956.8, 1899.9, 1950.0, 1889.3 cm^{-1}. ^{1}H NMR (benzene-d_6, ambient): *isomer A* δ 5.05 (s, 1 H, overlap with signal from isomer B), 4.80 (s, 1 H), 4.15 (s, 5 H, C_5H_5), 2.79 (s, 1 H), 2.76 (s, 1 H), 1.93 (s, 3 H, CH_3), 1.60 (s, 3 H, CH_3), 1.46 (s, 1 H); *isomer* B δ 5.04 (s, 1 H, overlap with signal from isomer A), 4.95 (s, 1 H), 4.14 (s, 5 H, C_5H_5), 2.42 (s, 1 H), 1.73 (s, 3 H, CH_3), 1.64 (s, 3 H, CH_3), 1.18 (s, 1 H), 0.35 (s, 1 H). ^{13}C NMR (benzene-d_6, ambient): *isomer A* δ 253.31 (s, 1 C, CO), 251.98 (s, 1 C, CO), 144.81 (s, 1 C), 133.72 (t, 1 C, J = 157.5 Hz), 90.80 (s, 1 C), 88.57 (d of qnt, 5 C, C_5H_5, J = 177.3, 6.4 Hz), 69.16 (d, 1 C, J = 150.5 Hz), 46.98 (t, 1 C, J = 156.6 Hz), 25.61 (q, 1 C, J = 125.5 Hz), 21.65 (q, 1 C, J = 127.0 Hz); *isomer B* δ 249.31 (s, 1 C, CO), 247.00 (s, 1 C, CO), 143.60 (s, 1 C), 115.72 (t, 1 C, J = 153.8 Hz), 101.83 (s, 1 C), 89.02 (d of qnt, 5 C, C_5H_5, J = 176.0, 6.2 Hz), 75.10 (d, 1 C, J = 157.3 Hz), 45.91 (t, 1 C, J = 159.6 Hz), 24.44 (q, 1 C, J = 126.3 Hz), 22.47 (q, 1 C, J = 127.0 Hz).

Cp*(C_5H_7)Cr(CO)$_2$ (7i) was isolated as bright orange-yellow needles from hexane and purified by recrystallization from hexane. Yield: 72%. Mp: 162–163 °C. FT-IR (hexane): 1934.6, 1873.8 cm^{-1}. Anal. Calcd for $C_{17}H_{22}CrO_2$: C, 65.79; H. 7.14. Found: C, 65.31; H, 7.21. ^{1}H NMR (benzene-d_6, ambient): δ 5.72 (dt, 1 H, H5, J = 10.5, 16.8 Hz), 5.30 (dd, 1 H, H6, J = 16.8, 1.8 Hz), 4.91 (dd, 1 H, H7, J = 9.9, 1.8 Hz), 3.05 (dt, 1 H, H3, J = 6.9, 10.2 Hz), 1.90 (dd, 1 H, H1, J = 6.9, 2.1 Hz), 1.64 (apparent t, 1 H, H4, J = 10.5 Hz), 1.42 (s, 15 H, C_5Me_5), 0.85 (dd, 1 H, H2, J = 9.6, 2.1 Hz). ^{13}C NMR (benzene-d_6, ambient): δ 251.34 (s, 1 C, CO), 248.80 (s, 1 C, CO), 136.69 (d, 1 C, J = 150.2 Hz), 112.79 (t, 1 C, J = 156.7 Hz), 98.91 (s, 5 C, C_5Me_5), 78.62 (d, 1 C, J = 161.0 Hz), 73.16 (d, 1 C, J = 160.0 Hz), 46.77 (t, 1 C, J = 159.3 Hz), 9.97 (q, 5 C, C_5Me_5, J = 126.6 Hz).

Cp(η^3-1,5-(Si(CH_3)$_3$)$_2$C$_5$H$_5$)Cr(CO)$_2$ (5i). This compound was prepared by the same procedure used for compounds **1i** and **7i**. It was isolated as orange needles from hexane and purified by recrystallization from hexane. Yield: 83%. Mp: 86–88 °C. FT-IR (hexane): 1947.1, 1887.3 cm^{-1}. Anal. Calcd for $C_{18}H_{28}CrO_2Si_2$: C, 56.22; H, 7.34. Found: C, 56.04; H, 7.67. ^{1}H NMR (benzene-d_6, ambient): δ 6.14 (d, 1 H, J = 18.3 Hz), 6.02 (dd, 1 H, J = 18.5, 9.5 Hz), 4.22 (s, 5 H, C_5H_5), 4.17 (dd (obscured by the Cp), 1 H, J = 10.5, 11.7 Hz), 1.84 (apparent t, 1 H, J = 9.5 Hz), 0.16 (s, 9 H, $SiMe_3$), 0.13 (s, 9 H, $SiMe_3$), –0.13 (d, 1 H, J = 12.6 Hz). ^{13}C NMR (benzene-d_6, ambient): δ 249.87 (s, 1 C, CO), 249.69 (s, 1 C, CO), 146.47 (d, 1 C, J = 152.9 Hz), 128.72 (d, 1 C, J = 140 Hz), 88.07 (d of qnt, 5 C, C_5H_5, J = 176.2, 6.8 Hz), 79.90 (d, 1 C, J = 160.5 Hz), 75.01 (d, 1 C, J = 160.6 Hz), 52.70 (d, 1 C, J = 140.0 Hz), 0.39 (q, $SiMe_3$, J = 119.3 Hz), –0.85 (q, $SiMe_3$, J = 118.9 Hz).

Cp(C_5H_7)Cr(DMPE) (1j). A 0.46-g (2.5-mmol) sample of **1** was dissolved in 15 mL of hexane, and then 0.45 mL (2.7 mmol) of 1,2-bis(dimethylphosphino)ethane (DMPE) was added to the solution by

Table I. X-ray Data Collection Parameters for $Cp^*(C_5H_7)Cr$ (A), $(Cp(C_5H_7)Cr[CN(2,6\text{-}(CH_3)_2C_6H_3)]$ (**B**), and $Cp(\eta^3\text{-}C_5H_7)Cr(CO)_2$ (C)

	A	B	C
formula	$CrC_{15}H_{22}$	$CrC_{19}H_{21}N$	$CrC_{12}H_{12}O_2$
mol wt	254.34	315.38	240.22
space group	$P2_1/n$	$P2_1/n$	$Pna2_1$
a, Å	7.593 (3)	10.379 (2)	19.653 (6)
b, Å	23.073 (7)	7.629 (2)	6.545 (2)
c, Å	8.530 (4)	19.961 (4)	17.126 (5)
β, deg	113.76 (2)	93.88 (2)	90
V, Å	1367.7	1576.9	2202.9
Z	4	4	8
d_{calc}, g/cm^3	1.24	1.33	1.45
λ	0.71073	0.71073	0.71073
temp, °C	16	16	16
cryst size, mm	0.28 × 0.23 × 0.15	0.38 × 0.30 × 0.15	0.34 × 0.25 × 0.16
linear abs coeff, cm^{-1}	7.90	7.00	9.89
scan type	θ–2θ	θ–2θ	θ–2θ
scan speed, deg/min	3–8	3–8	2.5–8
abs treatment	ψ scan	ψ scan	ψ scan
transmissn factors	0.917–1.000	0.875–1.000	0.823–1.000
scan range, deg	±1	±1	±1
2θ limits, deg	2.5–4.3	2.4–48	2–47
min *hkl*	0,0–8	0,0–22	0,0,0
max *hkl*	7,23,8	11,8,22	24,8,21
no. of unique obsd data	986	1653	1000
no. of variables	145	190	200
$R(F)$	0.047	0.048	0.052
$R_w(F)$	0.052	0.052	0.053
max diff Fourier peak, e/Å^3	0.38	0.29	0.57

syringe, resulting in the formation of dark red crystals in 10–15 min. The dark red product was isolated and dried under vacuum. The product was purified by recrystallization from ca. 15 mL of toluene at −20 °C and isolated as dark red needles. Yield: 46% (0.38 g). Mp: 103–107 °C. Anal. Calcd for $C_{16}H_{28}CrP_2$: C, 57.48; H, 8.44. Found: C, 57.41; H, 8.71. ^{1}H NMR (benzene-d_6, ambient): δ 5.34 (dt, 1 H, J = 9.9, 16.8 Hz), 4.95 (d, 1 H, J = 15.3 Hz), 4.71 (d, 1 H, J = 9.0 Hz), 3.76 (s, 5 H, C_5H_5), 3.56 (dt, 1 H, J = 6.3, 10.5 Hz), 2.48 (m, 1 H), 2.07 (dd, 1 H, J = 12.3, 6.0 Hz), 1.87 (dd, 1 H, J = 4.8, 9.3 Hz), 1.17 (d, 1 H, $J_{P\text{-}H}$ = 6.6 Hz), 1.03 (d, 1 H, $J_{P\text{-}H}$ = 6.6 Hz), 0.95 (d, 3 H, CH_3, $J_{P\text{-}H}$ = 6.6 Hz), 0.86 (d, 3 H, CH_3, $J_{P\text{-}H}$ = 6.6 Hz), 0.81 (d, 1 H, $J_{P\text{-}H}$ = 6.9 Hz), 0.68 (d, 1 H, $J_{P\text{-}H}$ = 6.0 Hz), 0.61 (apparent t, 6 H, CH_3, $J_{P\text{-}H}$ = 6.3 Hz). ^{13}C NMR (benzene-d_6, ambient): δ 146.0 (d, 1 C, J = 146.6 Hz), 100.15 (t, 1 C, J = 151.6 Hz), 85.52 (d of qnt, 5 C, C_5H_5, J = 171.2, 6.3 Hz), 76.61 (d, 1 C, J = 161.2 Hz), 58.16 (d, 1 C, J = 148.0 Hz), 35.62 (t, 1 C, J = 152.0 Hz), 30.65 (m, DMPE), 19.62 (m, DMPE), 12.8 (m, DMPE).

Vanadium Analogues. $Cp(1,5\text{-}(Me_3Si)_2C_5H_5)V(PEt_3)$. A solution of 0.26-g (0.61-mmol) of $CpVCl_2(PEt_3)_2$[12] in 30 mL of THF was reduced with Zn dust to $[CpVCl(PEt_3)]_2$ under reflux. The purple solution was then cooled to −78 °C, and a solution of 0.20 g (0.80 mmol) of K(1,5-$(SiMe_3)_2C_5H_5$) in 30 mL of THF was added dropwise with stirring. The mixture was warmed to room temperature slowly and stirred overnight, resulting in a dark brown solution. After the solvent was removed in vacuo, the product was extracted with 3 × 20 mL portions of hexane. The dark brown solution was filtered under nitrogen which produced traces of a deep purple product under positive pressure of nitrogen. The solution volume was reduced in vacuo to 20 mL and cooled to −86 °C, yielding 0.22 g (ca. 80%) of dark brown crystals. The extremely air- and moisture-sensitive product (mp 79–85 °C) was purified by recrystallization from hexane. The product readily lost PEt_3 under vacuum, and hence, sublimation could not be used for purification. Magnetic susceptibility (THF, 21.0 °C): 1.63 μ_B. EPR data (toluene, ambient, excess PEt_3): g = 1.977 + 0.001, A_V = 74.0 ± 0.3 G, A_P = 28.2 ± 0.3 G. Anal. Calcd for $C_{22}H_{43}Si_2PV$: C, 59.29; H, 9.72. Found: C, 59.06; H, 9.11.

$Cp(1,5\text{-}(Me_3Si)_2C_5H_5)V$. The blood red solution produced by dissolving 0.50 g (1.4 mmol) of $CpVI_2$[13] in 30 mL of THF was reduced with 0.053 g (0.81 mmol) of Zn dust. After the solution was stirred for 3 h at room temperature, the violet CpVI(THF) complex was apparently formed. The violet solution was cooled to −78 °C, and a solution of 0.37 g (1.5 mmol) of K(1,5-$(SiMe_3)_2C_5H_5$) dissolved in 25 mL of THF was added dropwise with stirring. The solution was warmed to room temperature slowly and stirred overnight, yielding a dark brown solution. The solvent was removed in vacuo, and the product was extracted with 3 × 25 mL portions of hexane. The black-brown solution was filtered under nitrogen or argon, producing a deep purple product under a positive pressure of nitrogen or argon. The solution was reduced in vacuo to 10 mL and cooled to −86 °C, yielding dark crystals. After three recrystallizations from hexane, 0.22 g (ca. 45%) of the extremely air- and moisture-sensitive product (mp 110–112 °C) was isolated. Sublimation of the product in vacuo at 75 °C produced golden crystals. The golden crystals turned purple under nitrogen and produced purple solutions. Magnetic susceptibility (THF, 27.0 °C): 1.3 μ_B. EPR data (toluene, ambient): g = 1.977 ± 0.001, A_V = 63.4 ± 0.2 G. Anal. Calcd for $C_{16}H_{28}Si_2V$: C, 58.68; H, 8.62; N, 0.00. Found: C, 58.55; H, 8.73; N, 0.00.

$Cp(1,5\text{-}(Me_3Si)_2C_5H_5)V(CO)$. Either of the previous two vanadium compounds was dissolved in a small volume of pentane and exposed to CO, whereupon the solution rapidly became a deep orange-red color. The compound did not always crystallize readily, particularly in the presence of PEt_3. If the PEt_3 complex was used for the preparation, the solvent and the phosphine were removed under high vacuum over the course of 1 day or so, and the crude product was redissolved in a small volume of pentane. After the concentrated solution was cooled to −78 °C overnight, a semicrystalline product was isolated, the yield of which was primarily limited by the product's solubility. IR data (solution): ν_{CO} = 1938 cm^{-1} ($\nu_{^{13}CO}$ = 1895 cm^{-1}). ESR data (toluene, room temperature): g = 1.990 ± 0.001, A_V = 67.1 ± 0.2 G. For the ^{13}CO analogue, no ^{13}C (I = 1/2) coupling was observed.

X-ray Structural Studies. Single crystals of each of the described compounds were obtained by slow cooling of their concentrated solutions utilizing the solvents mentioned in their preparations. Data were collected with use of a Nicolet P$\bar{1}$ autodiffractometer with accompanying software. All calculations employed the Enraf-Nonius SDP programs. Direct methods were used to find the approximate locations of the chromium (and several lighter) atoms, after which the remaining non-hydrogen atoms were found readily from difference Fourier maps. In subsequent refinements of positional parameters the function $\sum w(|F_o| - |F_c|)$ was minimized. Once the non-hydrogen atom locations had nearly refined to convergence, difference Fourier maps were used to locate the hydrogen atoms for all but the dicarbonyl structure. These atoms were included in these positions but were not refined. All structural solutions and refinements proceeded routinely. Other pertinent parameters relating to the data collection and refinement are provided in Table I.

Kinetic Studies. Decalin, used for all kinetic studies, was purified by letting it stand 1 day or longer over concentrated H_2SO_4 and then poured over KOH for 1 day, saturated with N_2, and distilled from Na/benzophenone. The ^{13}CO was obtained from Cambridge Isotopes and contained <1% ^{12}CO. Solution IR spectra were recorded in septum-sealed N_2-purged NaCl cells on a Nicolet FTIR 7199 spectrometer. Constant temperatures (±0.2 °C) for kinetic studies were maintained with a Haake Model F circulator. Solutions for ligand substitution studies were kept

(12) (a) Nieman, J.; Scholtens, H.; Teuben, J. H. *J. Organomet. Chem.* **1980**, *186*, C12. (b) Nieman, J.; Teuben, J. H.; Huffman, J. C.; Caulton, K. G. *J. Organomet. Chem.* **1983**, *255*, 193. (c) Nieman, J.; Teuben, J. H. *Organometallics* **1986**, *5*, 1149.

(13) King, R. B.; Hoff, C. D. *J. Organomet. Chem.* **1982**, *225*, 245.

in the dark, as some reactions could proceed predominantly via photolysis, particularly at the lower temperatures.

The compounds $Cp(C_5H_7)Cr^{13}CO$, $Cp^*(C_5H_7)Cr^{13}CO$, $Cp(2,4\text{-}C_7H_{11})Cr^{13}CO$, and $Cp((1,5\text{-}Me_3Si)_2C_2H_5)Cr^{13}CO$ were prepared from their half-open metallocenes as described above. The IR spectral bands (ν_{CO} (cm^{-1})) are observed for $Cp(C_5H_7)Cr^{13}CO$ at 1871; $Cp^*(C_5H_7)Cr^{13}CO$ at 1854; $Cp(2,4\text{-}C_7H_{11})Cr^{13}CO$ at 1868; $Cp(1,5\text{-}(Me_3Si)_2C_5H_5)Cr^{13}CO$ at 1871; $Cp^*(3\text{-}C_6H_9)Cr^{13}CO$ at 1855; and $Cp\text{-}(1,5\text{-}(Me_3Si)_2C_5H_5)V^{13}CO$ at 1895 in decalin. The CO exchange reactions were carried out in the dark in a rapidly agitated solution in an atmosphere of different partial pressures of CO. Three standardized tanks of CO (Matheson) containing 99.99% CO, 9.992% CO in N_2, and 1.002% CO in N_2 were used. Other mixtures were obtained by mixing the calibrated standard with N_2 by using a Matheson gas mixer and rotameter.

General procedures were similar to those already outlined in a previous publication.[4a] Degassed decalin was saturated with ^{12}CO, and a small aliquot of a stock solution of the ^{13}CO labeled complex was added via syringe. Aliquots for IR analysis were withdrawn in a similar manner, and then progress of the reaction was monitored by the increase in the IR carbonyl resonance of $(\eta^5\text{-}L)_2M^{12}CO$ and the decrease in absorbance of $(\eta^5\text{-}L)_2M^{13}CO$ as the mixture approached equilibrium. Data were analyzed by using a version of the McKay equation (eq 1) as previously

$$\ln\left(\frac{A - A_\infty}{A_0 - A_\infty}\right) = -k_1\left(\frac{[MCO]}{C} + 1\right)t \qquad (1)$$

described.[4a] A is the $(\eta^5\text{-}L)_2M^{13}CO$ absorbance, and k_1 is the CO independent rate constant. [MCO] represents the total metal carbonyl concentration. At the high concentrations of CO used in the kinetic studies $[MCO]/C$ is small and is given by $A_{M^{13}CO}/A_{M^{12}CO}$. A plot of the quantity on the left-hand side of eq 1 vs time gives a straight line (correlation coefficient ≥ 0.995) with the slope being k_{obsd}.

Results and Discussion

Synthetic, Spectroscopic, and Structural Studies. Half-Open Chromocenes. The reactions of "$CrCl_2$" with 1 equiv each of NaCp or KCp* and various potassium pentadienides lead to the selective formation of "half-open chromocenes" (eqs 2 and 3). The "$CrCl_2$"

$$\text{"}CrCl_2\text{"} + NaCp + KPdl \xrightarrow{\text{THF, "}ZnCl_2\text{"}} Cp(Pdl)Cr + NaCl + KCl \qquad (2)$$

Pdl = C_5H_7, 2,4-C_7H_{11},[9] 1,5-$(Me_3Si)_2C_5H_5$, 1,5-$(C_6H_5)_2C_5H_5$

$$\text{"}CrCl_2\text{"} + KC_5Me_5 + KPdl \xrightarrow{\text{THF, "}ZnCl_2\text{"}} Cp^*(Pdl)Cr + 2KCl \qquad (3)$$

Pdl = C_5H_7, 3-C_6H_9, 2,4-C_7H_{11}

employed in this reaction was prepared by the zinc reduction of $CrCl_3(THF)_3$, which may lead to a mixed-metal complex.[14] Interestingly, reactions with commercial $CrCl_2$ do not appear to be as selective, yielding significant quantities of chromocene and the respective open chromocene, indicating that the zinc presence may be largely responsible for the observed selectivity. Alternate routes in general were less convenient.

The half-open species bear some similarity to chromocene and the open chromocenes in that they are very air-sensitive (some even pyrophoric), volatile, monomeric complexes having two unpaired electrons. In color, the generally dark red half-open chromocenes much more closely resemble the scarlet chromocene than the deep green open chromocenes. Structural data demonstrate that these compounds exist in a normal half-open metallocene structure (similar to I or II, vide infra).

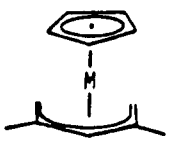

I

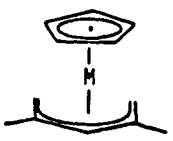

II

(14) (a) Bouma, R. J.; Teuben, J. H.; Beukema, W. R.; Bansemer, R. L.; Huffman, J. C.; Caulton, K. G. *Inorg. Chem.* **1984**, *23*, 2715. (b) Cotton, F. A.; Duraj, S. A.; Roth, W. J. *Inorg. Chem.* **1985**, *24*, 913.

Table II. Positional Parameters for the Non-Hydrogen Atoms in $Cp^*(C_5H_7)Cr$

atom	x	y	z
Cr	0.1909 (2)	0.13277 (5)	0.0740 (1)
C(1)	0.066 (1)	0.1180 (3)	0.252 (1)
C(2)	0.131 (1)	0.1751 (4)	0.2655 (9)
C(3)	0.0867 (9)	0.2139 (3)	0.127 (1)
C(4)	−0.005 (1)	0.1995 (4)	−0.049 (1)
C(5)	−0.091 (1)	0.1448 (4)	−0.113 (1)
C(6)	0.3567 (9)	0.1205 (3)	−0.0840 (8)
C(7)	0.2945 (8)	0.0663 (3)	−0.0484 (9)
C(8)	0.380 (1)	0.0579 (3)	0.130 (1)
C(9)	0.4933 (9)	0.1069 (4)	0.2035 (9)
C(10)	0.4801 (8)	0.1453 (3)	0.0712 (8)
C(11)	0.304 (1)	0.1457 (5)	−0.260 (1)
C(12)	0.173 (1)	0.0225 (5)	−0.177 (1)
C(13)	0.363 (1)	0.0029 (4)	0.222 (1)
C(14)	0.616 (1)	0.1149 (5)	0.390 (1)
C(15)	0.577 (1)	0.2033 (4)	0.089 (1)

Table III. Bond Distances (Å) and Angles (deg) for $Cp^*(C_5H_7)Cr$

Bond Distances			
Cr–C(1)	2.118 (7)	C(6)–C(7)	1.413 (8)
Cr–C(2)	2.103 (7)	C(7)–C(8)	1.406 (10)
Cr–C(3)	2.152 (6)	C(8)–C(9)	1.405 (9)
Cr–C(4)	2.102 (7)	C(9)–C(10)	1.405 (8)
Cr–C(5)	2.110 (6)	C(10)–C(6)	1.399 (8)
C(1)–C(2)	1.396 (10)	C(3)–C(4)	1.416 (10)
Cr–C(6)	2.202 (6)	C(6)–C(11)	1.504 (9)
Cr–C(7)	2.174 (6)	C(7)–C(12)	1.505 (10)
Cr–C(8)	2.175 (6)	C(8)–C(13)	1.526 (10)
Cr–C(9)	2.192 (6)	C(9)–C(14)	1.500 (9)
Cr–C(10)	2.225 (5)	C(10)–C(15)	1.503 (9)
C(2)–C(3)	1.410 (10)	C(4)–C(5)	1.426 (10)
Bond Angles			
C(1)–C(2)–C(3)	125.0 (7)	C(7)–C(8)–C(13)	125.1 (8)
C(7)–C(6)–C(10)	108.2 (6)	C(8)–C(9)–C(14)	125.5 (7)
C(6)–C(7)–C(8)	107.8 (6)	C(6)–C(10)–C(15)	125.0 (6)
C(7)–C(8)–C(9)	107.8 (6)	C(3)–C(4)–C(5)	124.6 (7)
C(8)–C(9)–C(10)	108.4 (6)	C(10)–C(6)–C(11)	126.4 (6)
C(6)–C(10)–C(9)	107.9 (5)	C(8)–C(7)–C(12)	125.3 (8)
C(2)–C(3)–C(4)	125.9 (6)	C(9)–C(8)–C(13)	127.0 (8)
C(7)–C(6)–C(11)	125.3 (7)	C(10)–C(9)–C(14)	126.0 (7)
C(6)–C(7)–C(12)	126.7 (8)	C(9)–C(10)–C(15)	127.2 (6)

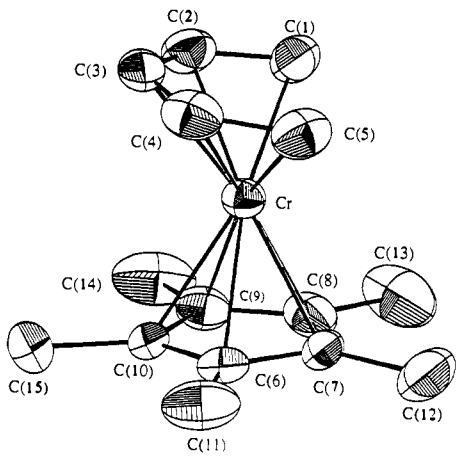

Figure 1. Perspective view and numbering scheme for $Cp^*(C_5H_7)Cr$.

The structural result for $Cp^*(C_5H_7)Cr$ may be seen in Figure 1, and pertinent bonding parameters are provided in Tables II and III. It can be seen that the complex does not adopt either an eclipsed (I) or a staggered (II) conformation, but instead is intermediate, being staggered by ca. 6°, as defined by the angle between the Cr–C(3)–(1/2C(1) + 1/2C(5)) and Cr–C(10)–(1/2C(7) + 1/2C(8)) planes (see supplementary material). In the related $Cp(2,4\text{-}C_7H_{11})M$ (M = Fe, Ru) structures,[5a,15] a

(15) Gleiter, R.; Hyla-Kryspin, I.; Ziegler, M. L.; Sergeson, G.; Green, J. C.; Stahl, L.; Ernst, R. D. *Organometallics* **1989**, *8*, 298.

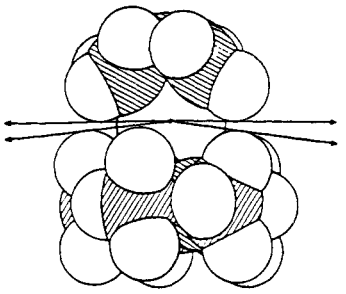

Figure 2. Space-filling model for $Cp^*(C_5H_7)Cr$.

crystallographically imposed mirror plane led to a corresponding angle of 0°. However, the Cp ligand carbon atoms exhibited large thermal parameters, suggesting that perhaps two slightly staggered conformations, like that found here, may actually have been present instead.

As the average Cr–C bond distances in chromocene[16] and the open chromocene,[3b] $(2,4\text{-}C_7H_{11})_2Cr$, have been found to be reasonably similar at 2.169 (4) and 2.163 (3) Å, respectively, one may not have expected to see much of a difference for the two ligands in a half-open chromocene. However, the average Cr–C(pentadienyl) distance of 2.117 (3) Å is clearly significantly shorter than the average Cr–C distance of 2.194 (3) Å for the Cp* ligand[17] and provides a further indication that at least the early transition metals bond more favorably to pentadienyl than to cyclopentadienyl ligands.[1a] The lengthening of the Cr–C(pentadienyl) bonds in $(2,4\text{-}C_7H_{11})_2Cr$ relative to $Cp^*(C_5H_7)Cr$ may readily be attributable, however, to the greater degree of steric crowding that characterizes pentadienyl ligands.[18] As can be seen in Figure 2, even though C_5H_7 is clearly much smaller than the C_5Me_5 ligand, it does possess a larger cone angle (ca. 180° vs 136° for Cp and 165° for Cp*).[18,19] This comes about as a result of geometric factors, most notably the relatively large C1–C5 separation of 2.917 Å, which for the Cp or Cp* ligands would instead be a much shorter bonding separation. To maintain similar M–C bond distances, a pentadienyl ligand plane must be closer to the metal atom, in this case 1.444 Å vs 1.838 Å for the Cp* ligand, and the effect is exacerbated for compounds having shorter bonds to the open Pdl ligand. This now seems to be a general trend for the larger transition metals, particularly the early ones. Thus, in both $Cp(C_5H_7)V(PEt_3)$ and $Cp(2,4\text{-}C_7H_{11})Ti(PEt_3)$ one sees similar behavior, with the M–C(pentadienyl) bond distances being shorter than those to the C_5H_5 ligands by ca. 0.092 (6) and 0.106 (5) Å, respectively.[20]

The Cr–C(pentadienyl) bond distances fall in three types. Those involving the 1- and 5-positions average 2.114 (5) Å, compared to 2.102 (5) Å for the 2- and 4-positions and 2.152 (6) Å for the 3-position. The two ligand planes, each defined by their five metal-bound atoms, are nearly planar, with the largest deviations being 0.043 and 0.005 Å for the open and closed ligands, respectively. For the open ligand, the formally uncharged carbon atoms (C(2,4)) experience slight deviations toward the metal, with the other carbon atoms deviating in the opposite direction.[21]

Mono(ligand) Adducts. Despite some similarities, there are also some very dramatic differences between the half-open chromocenes and their more symmetric analogues. In particular, while the 16-electron chromocene forms only a very weakly bound carbonyl adduct[22] and the open chromocenes do not seem to form any adducts at all, the half-open chromocenes form a variety of strongly bound adducts, Cp(Pdl)Cr(L), for L = CO, RNC, $P(OMe)_3$, $P(OCH_2)_3CCH_3$, and PF_3 (eqs 4–6). Adduct formation even

$$Cp(Pdl)Cr + L \rightarrow Cp(Pdl)Cr(L) \quad (4)$$

Pdl = C_5H_7, 3-C_6H_9, 2,3-C_7H_{11}, 2,4-C_7H_{11}, 1,5-$(Me_3Si)_2C_5H_5$, 1,5-$(C_6H_5)_2C_5H_5$; L = CO

Pdl = C_5H_7; L = PF_3, (t-C_4H_9)NC, 2,6-$(CH_3)_2C_6H_3NC$, $P(OMe)_3$, $P(OCH_2)_3CCH_3$

Pdl = 2,4-C_7H_{11}; L = (t-C_4H_9)NC

Pdl = 2,3-C_7H_{11}; L = $P(OCH_2)_3CCH_3$

$$Cp^*(Pdl)Cr + L \rightarrow Cp^*(Pdl)Cr(L) \quad (5)$$

Pdl = C_5H_7, 3-C_6H_9, 2,4-C_7H_{11}; L = CO

Pdl = C_5H_7; L = (t-C_4H_9)NC

$$[1,3\text{-}(Me_3Si)_2C_5H_3](C_5H_7)Cr + CO \rightarrow [1,3\text{-}(Me_3Si)_2C_5H_3](C_5H_7)Cr(CO) \quad (6)$$

with dimethylphenylphosphine may be observed, although in this case the process is readily reversible. The stronger ligand binding by the half-open chromocenes might well be attributable to the fact that both the metallocenes and the open metallocenes must undergo significant structural reorganization for ligand coordination to take place. The former must adopt a bent metallocene configuration (III), while the latter must generally adopt a syn-eclipsed conformation (IV),[23] both processes being unfavorable.[2a,24] In contrast, little reorganization is required in general for ligand coordination to a half-open metallocene such as I or II.

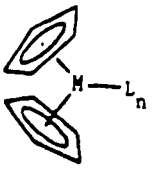

III

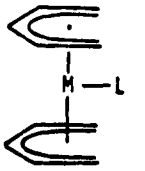

IV

The 18-electron half-open chromocene ligand adducts are diamagnetic, and their ^1H and ^{13}C NMR spectra revealed that these species were quite unusual, as the pentadienyl ligands displayed no symmetry whatsoever, unlike related complexes of titanium and vanadium. The spectra were reminiscent of those for $(\eta^5\text{-}2,4\text{-}C_7H_{11})_2Mo(PEt_3)$,[23] which was found to have one of its pentadienyl ligands attached in the highly unusual η^5-S (S = sickle) configuration. The half-open chromocene adducts were therefore assigned related structures (e.g., V), as opposed to the more normal arrangement found for the titanium and vanadium analogues (VI). This assignment was ultimately confirmed

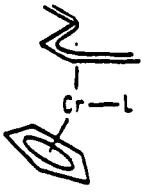

V

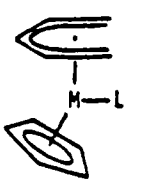

VI

crystallographically for a 2,6-xylyl isocyanide adduct (vide infra).

(16) Gard, E.; Haaland, A.; Novak, D. P.; Seip, R. *J. Organomet. Chem.* **1975**, *88*, 181.

(17) The standard deviations accompanying average values reflect the uncertainties of the average values, but not necessarily the distributions of the individual values.

(18) Stahl, L.; Ernst, R. D. *J. Am. Chem. Soc.* **1987**, *109*, 5673.

(19) Tolman, C. A. *Chem. Rev.* **1977**, *77*, 313.

(20) (a) Gedridge, R. W.; Hutchinson, J. P.; Ernst, R. D. Unpublished results. (b) Melendez, E.; Arif, A. M.; Ziegler, M. L.; Ernst, R. D. *Angew. Chem., Int. Ed. Engl.* **1988**, *27*, 1099.

(21) The deviation of the carbon atoms in the 2- and 4-positions is quite common, regardless of the substitution pattern. It may be related to the fact that the 2- and 4-substituents have a much greater tendency to tilt toward the metal center, and thereby pull their attached carbon atoms along somewhat as well.

(22) Wong, K. L. T.; Brintzinger, H. H. *J. Am. Chem. Soc.* **1975**, *97*, 5143.

(23) Stahl, L.; Hutchinson, J. P.; Wilson, D. R.; Ernst, R. D. *J. Am. Chem. Soc.* **1985**, *107*, 5016.

(24) Brintzinger, H. H.; Schwemlein, H.; Zsolnai, L.; Huttner, G. *J. Organomet. Chem.* **1983**, *256*, 285.

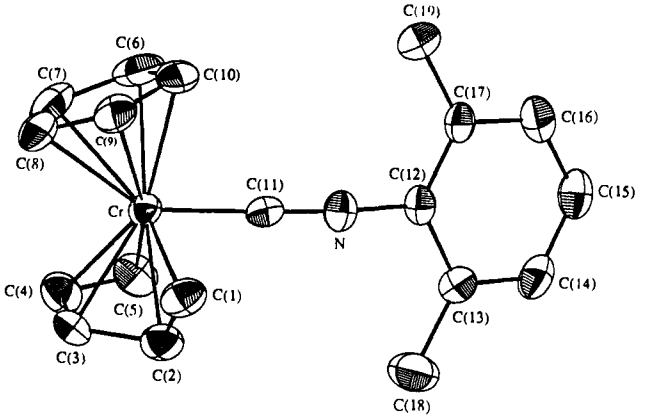

Figure 3. Perspective view and numbering scheme for $Cp(C_5H_7)Cr[CN-[2,6-(CH_3)_2C_6H_3]]$.

A similar coordination environment has also subsequently been proposed for related molybdenum complexes,[25] and η^5-S coordination, while still very rare, has also been reported for a (dienyl)$W(CO)_3Br$[26] and a (Cp*)(dienyl)$ReCl$[27] complex. Notably, all of these may be regarded as possessing both d^4 and 18-electron configurations, although these properties do not by themselves guarantee η^5-S coordination (cf. $(2,4\text{-}C_7H_{11})Mo(CO)_3I$).[28]

The presence of an η^5-S, as opposed to η^5-U, bound pentadienyl ligand in these adducts leads to the possible existence of two diastereomers for unsymmetrically substituted pentadienyl groups. In fact, for $Cp(2,3\text{-}C_7H_{11})Cr(CO)$, two isomers were indeed observed spectroscopically, one significantly more abundant than the other. These may readily be assigned structures VII and VIII.

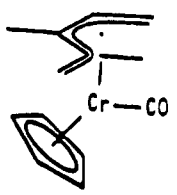

VII

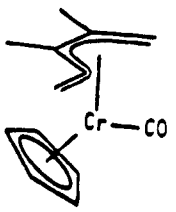

VIII

As the former structure seems to possess significantly greater intramolecular nonbonded repulsions involving its 2-methyl substituent, it would be expected to be the minor (less stable) isomer, which is in accord with the NMR assignments. In fact, there is further evidence to substantiate this assignment. In the case of $Cp(\eta^5\text{-}S\text{-}2,4\text{-}C_7H_{11})Cr(CO)$, there will necessarily be one methyl group oriented toward the CO ligand, which should therefore destabilize the adduct. Indeed, this adduct is significantly more difficult to prepare relative to the other PdI analogues and is also far more prone to losing CO. Hence, the presence of a 2-methyl substituent on the handle end of the η^5-sickle does lead to significant destabilization.

A structural study on $Cp(C_5H_7)Cr$(2,6-xylyl isocyanide) (Figure 3, Tables IV and V) has indeed confirmed that the η^5-S mode of the pentadienyl ligation is again present. In this regard, the C(1)–C(2)–C(3)–C(4) torsion angle was found to be 123.4 (6)°, indicating a twist of the C(1)–C(2) vector out of the C(2)–C(3)–C(4)–C(5) plane by 56.6°. Similarly, while the C(2)–C(5) atoms lie in a well-defined plane (the largest deviation being 0.001 Å), C(1) is found 1.061 (6) Å out of this plane, leading to a related angle of 49.8°. It can be noted that the corresponding angles for the related Mo and W sickle compounds were smaller, which seems reasonable since more bending should be required for the smaller metal to bring the sickle handle into bonding proximity. Additionally, the C–C–C(pentadienyl) bond angles average significantly less than 120°, presumably again to promote more effective M–pentadienyl interactions. Despite the significant nonplanarity of the C_5H_7 ligand, there seems to be little evidence of allyl-ene coordination (IX), as invoked in other cases.[25-27] Thus, the C–C(pentadienyl) distances are somewhat similar, ranging from 1.389 (7) to 1.437 (7) Å. The terminal C–C distances follow the normal trend of being shorter than the internal ones, due to a contribution by hybrid X. However, it might be that the simultaneous participation of two allyl-ene hybrids, IX and XI, could lead to the observed pattern.

IX

As expected, the C_5H_5 carbon atoms are nearly planar, the greatest deviation being 0.003 Å. This plane is tilted 23.0 (6)° from the C(2)–C(5) plane. The Cr–C(11) vector is nearly parallel to the C(2)–C(5) plane (tilted by 5.6°) but experiences a greater

Table IV. Positional Parameters for the Non-Hydrogen Atoms in $Cp(C_5H_7)Cr[CN(2,6\text{-}(CH_3)_2C_6H_3)]$

atom	x	y	z
Cr	0.35639 (8)	0.2017 (1)	0.11552 (4)
N	0.2130 (4)	0.0945 (6)	−0.0168 (2)
C(1)	0.2288 (6)	0.4365 (8)	0.1154 (3)
C(2)	0.3392 (6)	0.4580 (8)	0.0806 (3)
C(3)	0.4573 (6)	0.4379 (8)	0.1218 (3)
C(4)	0.5448 (6)	0.3100 (9)	0.1014 (3)
C(5)	0.5138 (5)	0.2125 (9)	0.0438 (3)
C(6)	0.3617 (7)	−0.0700 (8)	0.1470 (3)
C(7)	0.4548 (6)	0.0234 (9)	0.1874 (3)
C(8)	0.3893 (6)	0.1475 (8)	0.2243 (3)
C(9)	0.2579 (6)	0.1303 (8)	0.2073 (3)
C(10)	0.2393 (6)	−0.0009 (8)	0.1601 (3)
C(11)	0.2696 (5)	0.1379 (7)	0.0337 (2)
C(12)	0.1740 (5)	0.0218 (7)	−0.0783 (3)
C(13)	0.6872 (5)	0.3766 (8)	0.3630 (3)
C(14)	0.6522 (6)	0.4553 (9)	0.3015 (3)
C(15)	0.6043 (6)	0.6251 (9)	0.2987 (3)
C(16)	0.5902 (5)	0.7177 (9)	0.3564 (3)
C(17)	0.1251 (5)	−0.1476 (7)	−0.0808 (3)
C(18)	0.7395 (7)	0.1955 (9)	0.3683 (3)
C(19)	0.1103 (6)	−0.2483 (8)	−0.0175 (3)

Table V. Bond Distances (Å) and Angles (deg) for $Cp(C_5H_7)Cr[CN(2,6\text{-}(CH_3)_2C_6H_3)]$

Bond Distances

Cr–C(1)	2.228 (5)	Cr–C(8)	2.215 (5)	C(12)–C(13)	1.419 (7)
Cr–C(2)	2.080 (5)	Cr–C(9)	2.226 (4)	C(14)–C(15)	1.387 (7)
Cr–C(3)	2.084 (5)	Cr–C(10)	2.192 (5)	C(17)–C(12)	1.388 (6)
Cr–C(4)	2.159 (5)	C(13)–C(14)	1.393 (6)	C(6)–C(7)	1.410 (8)
Cr–C(5)	2.246 (5)	C(16)–C(17)	1.388 (6)	C(7)–C(8)	1.403 (7)
Cr–C(11)	1.876 (5)	C(17)–C(19)	1.496 (6)	C(8)–C(9)	1.389 (7)
N–C(11)	1.178 (5)	C(1)–C(2)	1.389 (7)	C(9)–C(10)	1.380 (7)
N–C(12)	1.384 (6)	C(2)–C(3)	1.437 (7)	C(10)–C(6)	1.416 (8)
Cr–C(6)	2.165 (5)	C(3)–C(4)	1.412 (7)	C(15)–C(16)	1.368 (7)
Cr–C(7)	2.181 (5)	C(4)–C(5)	1.390 (7)	C(13)–C(18)	1.485 (8)

Bond Angles

C(1)–C(2)–C(3)	113.7 (4)	N–C(12)–C(17)	119.3 (4)
C(2)–C(3)–C(4)	116.7 (4)	C(13)–C(12)–C(17)	122.3 (4)
C(3)–C(4)–C(5)	119.4 (5)	C(12)–C(13)–C(18)	120.3 (4)
C(6)–C(7)–C(8)	107.7 (5)	C(12)–C(17)–C(19)	120.4 (4)
C(7)–C(8)–C(9)	108.1 (5)	C(18)–C(13)–C(14)	122.4 (4)
C(8)–C(9)–C(10)	109.0 (5)	C(19)–C(17)–C(16)	122.0 (4)
C(9)–C(10)–C(6)	108.1 (5)	C(12)–C(13)–C(14)	117.3 (4)
C(10)–C(6)–C(7)	107.2 (5)	C(13)–C(14)–C(15)	120.6 (5)
Cr–C(11)–N	178.1 (4)	C(14)–C(15)–C(16)	120.5 (5)
C(11)–N–C(12)	166.1 (4)	C(15)–C(16)–C(17)	121.7 (5)
N–C(12)–C(13)	118.4 (4)	C(16)–C(17)–C(12)	117.6 (4)

(25) (a) Lee, G.-H.; Peng, S.-M.; Lee, T.-W.; Liu, R.-S. *Organometallics* **1986**, *5*, 2378. (b) Green, M.; Nagle, K. R.; Woolhouse, C. M.; Williams, D. J. *J. Chem. Soc., Chem. Commun.* **1987**, 1793.

(26) Sivavec, T. M.; Katz, T. J.; Chiang, M. Y.; Yang, X.-Q. *Organometallics* **1989**, *8*, 1620.

(27) Herrmann, W. A.; Fischer, R. A.; Herdtweck, E. *Organometallics* **1989**, *8*, 2821.

(28) Kralik, M. S.; Rheingold, A. L.; Ernst, R. D. Unpublished results.

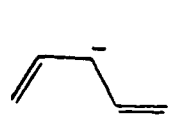

X

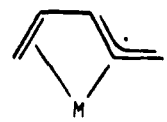

XI

tilt of 24.3° relative to the C_5H_5 plane. The Cr–C(Cp) bond distances average 2.196 (2) Å, although C(8) and C(9) seem lengthened perhaps due to their proximity to the pentadienyl handle. The average Cr–C(pentadienyl) distance of 2.159 Å is shorter, but is less meaningful due to the significant differences in the individual values. Notably, the shortest Cr–C(pentadienyl) interactions involve the three internal carbon atoms, indicating that the η^5-S coordination leads to some difficulties in bringing about simultaneous bonding between the metal atom and the two terminal pentadienyl carbon atoms, which are 3.780 Å apart. Relative to $Cp^*(C_5H_7)Cr$, ligand coordination significantly lengthens the $Cr–C(C_5H_7)$ distances. Interestingly, the 18-electron mono(ligand) adducts may be oxidized to cationic 17-electron species, for which structural results demonstrate normal η^5-U coordination. Hence, a very narrow window of stability seems to exist for the η^5-S coordination.[29]

Bis(ligand) Adducts. Interestingly, $Cp(2,4\text{-}C_7H_{11})Cr(CN(t\text{-}C_4H_9))$ is not stable at room temperature, undergoing disproportionation to a single isomer of $Cp(\eta^3\text{-}2,4\text{-}C_7H_{11})Cr(CN(t\text{-}C_4H_9))_2$ as the only observable diamagnetic product. This disproportionation (eq 7) thus converts $Cp(2,4\text{-}C_7H_{11})Cr(CN(t\text{-}C_4H_9))$, an 18-electron complex, to 16- and 18-electron species. Presumably the driving force is the relief of strain in the η^5-S coordination.

$$2Cp(2,4\text{-}C_7H_{11})Cr(CN(t\text{-}C_4H_9)) \rightarrow Cp(2,4\text{-}C_7H_{11})Cr + Cp(\eta^3\text{-}2,4\text{-}C_7H_{11})Cr(CN(t\text{-}C_4H_9))_2 \quad (7)$$

The half-open chromocene complexes could also undergo coordination by a second Lewis base (eqs 8–10), yielding complexes containing η^3-bound pentadienyl ligands. IR, ^1H, and ^{13}C NMR spectroscopy are all in accord with these formulations, and definitive confirmation was obtained through an X-ray diffraction study. In several cases, the presence of isomers could be detected

$$Cp^*(C_5H_7)Cr + 2CO \rightarrow Cp^*(\eta^3\text{-}C_5H_7)Cr(CO)_2 \quad (8)$$

$$Cp(Pdl)Cr + 2CO \rightarrow Cp(Pdl)Cr(CO)_2 \quad (9)$$

$$Pdl = C_5H_7,\ 2,4\text{-}C_7H_{11},\ 1,5\text{-}(Me_3Si)_2C_5H_5$$

$$Cp(C_5H_7)Cr + dmpe \rightarrow Cp(C_5H_7)Cr(dmpe) \quad (10)$$

spectroscopically. By analogy to the thoroughly investigated $Cp(allyl)M(L)_2$ parent species,[30] these complexes may be formulated as containing mixtures of endo (XII) and exo (XIII)

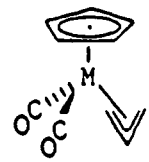

XII

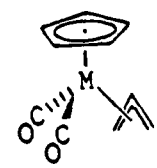

XIII

isomers. The relative proportions of these isomers were very sensitive to the conditions of preparation. Thus, while $Cp(\eta^3\text{-}C_5H_7)Cr(CO)_2$ and $Cp^*(\eta^3\text{-}C_5H_7)Cr(CO)_2$ were both isolated as single (exo) isomers, prolonged standing of at least the former in hexane solution led to the apparent formation of some of the endo isomer, with C–O stretching frequencies of 1880 and 1940 cm^{-1}. The formation of $Cp(\eta^3\text{-}2,4\text{-}C_7H_{11})Cr(CO)_2$ required much longer exposure to CO and resulted in two isomers, observed in both the IR and NMR spectra (see Experimental Section). In contrast, $Cp(\eta^3\text{-}C_5H_7)Cr(CN(t\text{-}C_4H_9))_2$ was isolated as a mixture of isomers regardless of the method of preparation, while $Cp(\eta^3\text{-}2,4\text{-}C_7H_{11})Cr(CN(t\text{-}C_4H_9))_2$ was formed almost exclusively as a single isomer in room-temperature reactions, although the higher temperature reactions led to a 60:40 ratio of isomers.

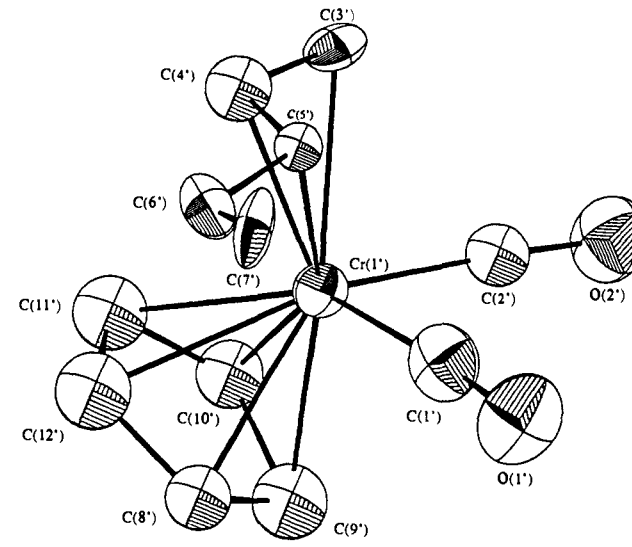

Figure 4. Solid-state structure of $Cp(\eta^3\text{-}C_5H_7)Cr(CO)_2$.

A solid-state structure determination has been carried out for $Cp(\eta^3\text{-}C_5H_7)Cr(CO)_2$ and confirms the foregoing conclusions (see Figure 4 and supplementary material). The quality of the structural result is not high, perhaps due to the presence of a noncrystallographic inversion center near 0.375, 0, 0. One must therefore be careful in interpreting the data. Nonetheless, these results clearly confirm the presence of η^3-pentadienyl coordination in the bis(ligand) adducts, and the general features are similar to those found in related $Cp(C_3H_5)M(CO)_2$ structures.[30] The exo orientation of the allyl fragment is clearly evident (Figure 4), and one finds average Cr–C(Cp) and Cr–CO bond distances of 2.21 (2) and 1.82 (2) Å, respectively.

Vanadium Analogues. In order that additional insight could be gained for the unusual kinetic data obtained for $Cp(1,5\text{-}(Me_3Si)_2C_5H_5)CrCO$ (vide infra), attempts were made to prepare its vanadium analogue by the general route employed for other vanadium complexes (eq 11). Unlike other half-open vanadocene

$$\tfrac{1}{2}[CpVCl(PEt_3)_2]_2 + K(1,5\text{-}(Me_3Si)_2C_5H_5) \rightarrow Cp(1,5\text{-}(Me_3Si)_2C_5H_5)V(PEt_3) + KCl \quad (11)$$

phosphine complexes, which exhibited 16-line patterns in their ESR spectra, a total of 24 lines were observed for this species. Addition of an excess of PEt_3 to this sample, however, led to a 16-line pattern (matching 16 of the 24 original peaks with g = 1.997, A_V = 74 G, and A_P = 28 G) quite similar to those observed for related phosphine complexes,[4a] suggesting that dissociation of PEt_3 was quite facile (eq 12) unlike all previously encountered

$$Cp(1,5\text{-}(Me_3Si)_2C_5H_5)V(PEt_3) \rightarrow Cp(1,5\text{-}(Me_3Si)_2C_5H_5)V + PEt_3 \quad (12)$$

half-open vanadocenes, in which an additional ligand appeared necessary for stability. Not surprisingly, then, it proved possible to prepare the phosphine-free complex (eq 13). Notably, this

$$CpVI(THF)_x + K(1,5\text{-}(Me_3Si)_2C_5H_5) \rightarrow Cp(1,5\text{-}(Me_3Si)_2C_5H_5)V + KI + x\text{THF} \quad (13)$$

species is low spin, like $(2,4\text{-}C_7H_{11})_2V$, but unlike Cp_2V which has three unpaired electrons. However, unusual color changes are observed for this species under various conditions (see Experimental Section), which may point to some unusual properties. Nonetheless, exposure of either of the above compounds to CO

(29) (a) The structural results and complementary kinetic studies will be reported shortly.[29b] (b) Shen, J. K.; Hallinan, N. C.; Freeman, J. W.; Arif, A. M.; Rheingold, A. L.; Ernst, R. D.; Basolo, F. Manuscript in preparation.

(30) (a) Faller, J. W.; Chodosh, D. F.; Katahira, D. *J. Organomet. Chem.* **1980**, *187*, 227. (b) Faller, J. W.; Ma, Y. *Organometallics* **1986**, *5*, 1949.

Table VI. Rates of CO Exchange for the Cr and V Compounds in Decalin at 1 atm of CO

compound	temp, °C	10^4[CO]	k_{obs}/f,[a] s^{-1}
$Cp^*(C_5H_7)CrCO$	51.0	57.2	8.93×10^{-5}
	60.0	56.7	2.92×10^{-4}
	70.0	56.1	6.51×10^{-4}
$Cp^*(3\text{-}C_6H_9)CrCO$[b]	27.3	58.6	3.51×10^{-6}
	36.9	58.0	1.47×10^{-5}
	46.7	57.5	5.26×10^{-5}
	54.8	57.0	1.56×10^{-4}
$Cp(C_5H_7)CrCO$	27.0	58.6	6.10×10^{-6}
	50.0	57.2	1.71×10^{-4}
	60.0	56.7	4.20×10^{-4}
	70.0	56.1	1.73×10^{-3}
$Cp(2,4\text{-}C_7H_{11})CrCO$[b]	30.0	58.4	1.18×10^{-4}
	40.0	57.8	4.01×10^{-4}
	50.0	57.2	1.26×10^{-3}
$Cp(1,5\text{-}(Me_3Si)_2C_5H_5)CrCO$	34.7	58.1	2.93×10^{-4}
	41.8	57.7	5.82×10^{-4}
	50.9	57.2	1.56×10^{-3}
$Cp(1,5\text{-}(Me_3Si)_2C_5H_5)VCO$	19.6	59.4	3.61×10^{-6}
	27.0	58.6	1.12×10^{-5}
	37.0	58.0	5.11×10^{-5}
	45.7	57.5	1.70×10^{-4}
	51.2	57.2	3.54×10^{-4}

[a] $f = [MCO]/C + 1$; $[MCO] \cong 5 \times 10^{-3}$ M. [b] The pentadienyls are 3-$CH_3C_5H_6$ and 2,4-$(CH_3)_2C_5H_5$, respectively.

Table VII. Activation Parameters of CO Exchange for the Cr and V Compounds in Decalin at 1 atm of CO

compound	$\Delta H^{\ddagger}$, kcal/mol	$\Delta S^{\ddagger}$, cal/(mol K)
$Cp^*(C_5H_7)CrCO$	22.8 ± 3.0	−7.9 ± 8.9
$Cp^*(3\text{-}C_6H_9)CrCO$[a]	26.2 ± 0.3	3.8 ± 1.0
$Cp(C_5H_7)CrCO$	25.9 ± 1.1	4.0 ± 3.5
$Cp(2,4\text{-}C_7H_{11})CrCO$[a]	22.4 ± 0.6	−2.8 ± 1.8
$Cp(1,5\text{-}(Me_3Si)_2C_5H_5)CrCO$	19.8 ± 1.1	−10.4 ± 3.4
$Cp(1,5\text{-}(Me_3Si)_2C_5H_5)VCO$	26.8 ± 0.1	8.2 ± 0.3

[a] The pentadienyls are 3-$CH_3C_5H_6$ and 2,4-$(CH_3)_2C_5H_5$, respectively.

leads to very rapid formation of the desired monocarbonyl complex (eq 14, $x = 0, 1$).

$$Cp(1,5\text{-}(Me_3Si)_2C_5H_5)V(PEt_3)_x + CO \rightarrow Cp(1,5\text{-}(Me_3Si)_2C_5H_5)V(CO) + xPEt_3 \quad (14)$$

Kinetic Studies. The half-open chromium carbonyl complexes all have higher CO stretching frequencies than the parent Cp_2CrCO (1900 cm^{-1}), indicating that the pentadienyl group appears to withdraw more electron density from Cr than does the cyclopentadienyl ligand. Unfortunately, the weak binding of CO to Cp_2Cr prevented any kinetic study being made on Cp_2CrCO.[22]

The CO exchange reaction (eq 15) can be followed by monitoring changes in the IR carbonyl absorbances of the CO and ^{13}CO labeled species. Observed rate constants k_{obsd} (s^{-1}) for exchange

$$(\eta^5\text{-L})_2Cr^{13}CO + CO \rightarrow (\eta^5\text{-L})_2CrCO + {}^{13}CO \quad (15)$$

reactions of the Cp(Pdl)CrCO, Cp^*(Pdl)CrCO, and Cp(1,5-$(Me_3Si)_2C_5H_5$)VCO complexes are given in Table VI, and the relevant activation data are shown in Table VII. Kinetic data for the exchange of CO with the ^{13}CO-labeled complexes were obtained in decalin at 27–70 °C.

Rate constants for the CO exchange reactions at 0.1 atm of partial pressure of CO were consistently lower than those obtained for 0.5 and 1.0 atm. Rate constants for the latter two pressures tended to be quite similar (Table VIII). Such CO dependencies are not consistent with a partial contribution of a second-order pathway, but rather indicate that diffusion of CO is retarding the rate of reaction at lower pressures. Indeed, at the higher temperatures, for which the more rapid reaction rates require faster CO diffusion, even the data for 0.5 atm start to be affected. In no case, however, did the reaction rates appear so rapid that the data at $P_{CO} = 1$ atm suffered noticeably. Thus, linear plots of $\ln(k/T)$ vs $1/T$ were observed for these data, which would not be expected were an associative pathway also participating.

Table VIII. Effect of CO Concentration on the Rates, k_{obsd}/f[a] (s^{-1}), of CO Exchange

	partial pressure of CO, atm		
temp, °C	0.1	0.5	1.0
(a) $Cp^*(3\text{-}C_6H_9)Cr^{13}CO$ in Decalin			
27.3	3.22×10^{-6}	3.44×10^{-6}	3.51×10^{-6}
36.9	1.39×10^{-5}	1.46×10^{-5}	1.47×10^{-5}
46.9	4.86×10^{-5}	5.56×10^{-5}	5.40×10^{-5}
56.6	1.5×10^{-4}	1.9×10^{-4}	1.8×10^{-4}
(b) $Cp(1,5\text{-}(SiMe_3)_2C_5H_5)V^{13}CO$ in Decalin			
19.6	3.60×10^{-6}	3.62×10^{-6}	3.61×10^{-6}
37.0	4.41×10^{-5}	5.08×10^{-5}	5.11×10^{-5}
45.7	1.25×10^{-4}	1.70×10^{-4}	1.70×10^{-4}
51.2	2.74×10^{-4}	3.36×10^{-4}	3.54×10^{-4}

[a] $f = [MCO]/C + 1$; $[MCO] \cong 5 \times 10^{-3}$ M.

Table IX. Rates and Activation Parameters of CO Addition to $Cp^*(C_5H_7)CrCO$ in Decalin at 1 atm of CO

temp, °C	k_{obsd}, s^{-1} [a]	$\Delta H^{\ddagger}$, kcal/mol	$\Delta S^{\ddagger}$, cal/(mol K)
70.0	2.41×10^{-5}	19.5 ± 1.2	−13 ± 3.3
80.0	4.81×10^{-5}		
90.0	1.20×10^{-4}		

[a] Dividing k_{obsd} by the molar solubility of CO at the different temperatures gives values of second-order rate constants k_2 (M^{-1} s^{-1}) of 3.88×10^{-3}, 8.17×10^{-3}, and 2.00×10^{-2}, respectively.

Therefore, the k_{obsd} values in Table VI are equal to first-order rate constants at a sufficiently high concentration of CO to render any CO diffusion retardation of rate negligible.

The CO addition reaction (eq 16) can also be conveniently monitored by IR spectroscopy. Kinetic data for the addition of CO to $Cp^*(C_5H_7)CrCO$ were obtained in decalin at 70–90 °C,

$$(\eta^5\text{-L})_2CrCO + CO \rightarrow (\eta^5\text{-L})(\eta^3\text{-L})Cr(CO)_2 \quad (16)$$

and rate constants and activation data are given in Table IX. The rate of CO addition is 1 order of magnitude slower than the rate of CO exchange and has a $\Delta H^{\ddagger} = 19.5 \pm 1.2$ kcal/mol and a $\Delta S^{\ddagger} = -13 \pm 3.3$ cal/(mol K). These values may reflect the η^5-η^3 transformation which presumably occurs in the transition state.

The 18-electron half-open complexes, CpPdlCrCO, are relatively inert, undergoing CO substitution at elevated temperatures by a predominantly dissociative mechanism. Although these complexes have the potential of undergoing associative attack at the metal because of the possibility of an η^5–η^3 bonding change occurring at either the cyclopentadienyl or the pentadienyl ligand, the kinetic data obtained suggest that such an internal bond change is not important in these systems and that significant M–CO bond cleavage in the transition state is occurring.

Mechanism of CO Exchange. The rates of CO exchange (eq 15) with 18-electron half-open chromocenes show no dependence on the concentration of CO at 0.5 and 1.0 atm of CO, indicating that the rate-determining step is first order in substrate concentration and zero order in CO concentration. This implies a dissociative pathway for CO exchange or substitution. From the structural and spectroscopic results reported herein, it appears that the dissociative reaction should involve the following conformation changes (eq 17), provided that no significant barrier exists to the η^5-S $\rightleftarrows$ η^5-U interconversions. In this light it is possible to suggest interpretations for the observed differences in exchange rates for the various half-open chromocene carbonyls. At 50 °C, the rates of reaction for the Cp(Pdl)CrCO complexes increase in the order C_5H_7 < 2,4-C_7H_{11} < 1,5-$(Me_3Si)_2C_5H_5$ (Table VI), which can be attributed to the usual steric acceleration for ligand substitution of metal complexes. For the 2,4-C_7H_{11} species, the presence of methyl groups in both the 2- and 4-positions ensures that one of them will point toward and weaken the metal–CO bond, while for the silylated compound, one or both of the very bulky Me_3Si substituents will reside near the carbonyl ligand and should also weaken the Cr–CO bond.

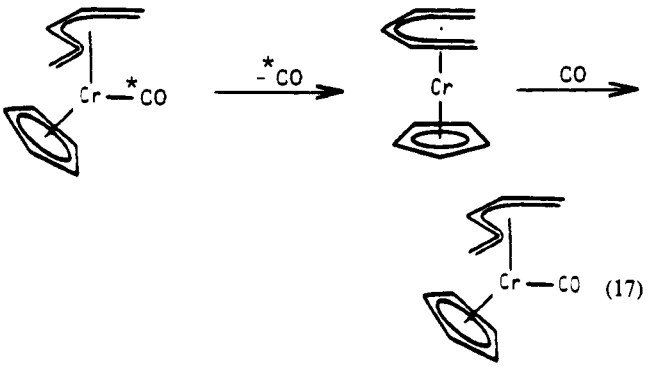

(17)

In accord with this idea, it can be noted that the value of $\Delta H^{\ddagger}$ (Table VII) for the $Cp(C_5H_7)CrCO$ complex is only slightly lower than that of its vanadium analogue (28.8 ± 0.3 kcal/mol), whereas the value for the 2,4-C_7H_{11} complex is significantly lower than that of its vanadium analogue (27.9 ± 0.8 kcal/mol). The smaller size of chromium and the presence of η^5-S coordination for its pentadienyl ligands should both lead to enhanced steric constraints in the chromium compound. The greater steric constraints of the Cr relative to the analogous V systems would weaken the Cr–CO bond and result in lower $\Delta H^{\ddagger}$ values of Cr relative to V.

There are other good reasons to expect both $\Delta H^{\ddagger}$ and $\Delta S^{\ddagger}$ to have small magnitudes. First, CO is bound only very weakly by chromocene, and not at all by the open chromocenes, so that the Cr–CO bond strength in the half-open chromocenes is not expected to be particularly strong. Additionally, a low value of $\Delta S^{\ddagger}$ could well arise from the fact that loss of CO from a half-open chromocene would lead to η^5-S to η^5-U conversion (eq 16), accompanied by an increase in order and symmetry and a decrease in entropy. Notably, the $\Delta S^{\ddagger}$ values observed here do seem smaller than the observed values (ca. 10 cal/(mol K)) for their vanadium counterparts. The value of $\Delta S^{\ddagger} = -10.4$ cal/(mol K) for $Cp(1,5\text{-}(Me_3Si)_2C_5H_5)CrCO$ is particularly strange, however, for a dissociative process, and so additional data were gathered for its vanadium analogue, $Cp(1,5\text{-}(Me_3Si)_2C_5H_5)VCO$. This compound displays much more reasonable values of $\Delta H^{\ddagger}$ (26.8 ± 0.1 kcal/mol) and $\Delta S^{\ddagger}$ (8.2 ± 0.3 cal/(mol K)) for a dissociative process that illustrates again the presence of a steric acceleration for the chromium complex ($\Delta H^{\ddagger} = 19.8 \pm 1.1$ kcal/mol). These data further support the proposition that the low $\Delta S^{\ddagger}$ value for the chromium analogue results from the η^5-S to η^5-U conformational change and is not just an artifact of the Me_3Si groups. In contrast to the vanadium results, the CO substitution reactions for the chromium compounds do not simply involve CO coming off and on (eq 18). The η^5-S to η^5-U change must be quite

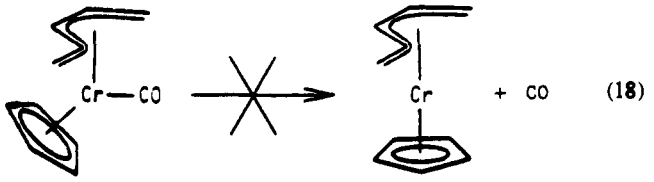

(18)

advanced in the transition state for reaction and probably promotes the CO release. Thus, the observed values of $\Delta H^{\ddagger}$ and $\Delta S^{\ddagger}$ may still be attributed to a classic dissociative type of process.

The values of the activation parameters for reactions of the Cp*PdlCrCO complexes are also enlightening. Despite the presence of five methyl substituents, no steric acceleration of the exchange reaction is apparent. Two factors could easily explain this. First, as noted in the structural discussion, separations between metal centers and Cp (or Cp*) ligands must be significantly longer than those to pentadienyl ligands as long as the average M–C bond distances are similar. Hence, the methyl groups are situated further from the metal coordination sphere and exhibit less steric repulsion (cf. Cp* cone angle of 165° vs 180–190° for pentadienyl ligands). In addition, the five methyl groups on the Cp* ligand lead to a much lower C–O stretching frequency (greater Cr–CO bond strength) than observed for the Cp analogue, which then opposes any sterically induced bond

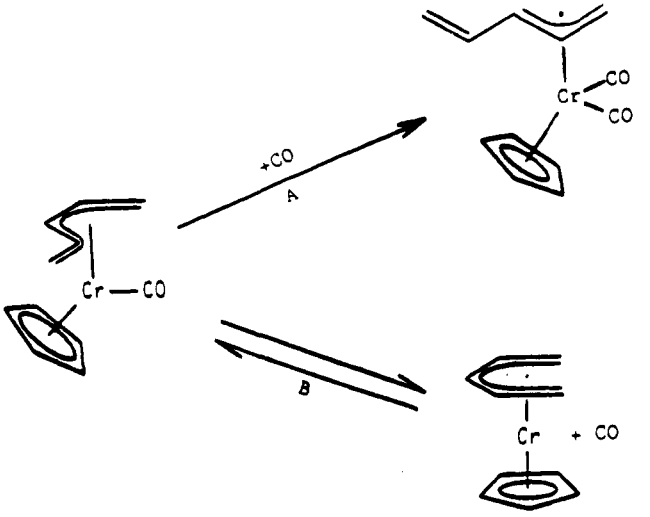

Figure 5. Proposed reaction pathways for (A) CO addition and (B) CO exchange.

weakening. In contrast, methylation on pentadienyl ligands brings about only meager reductions in the C–O stretching frequencies[1a] (see Experimental Section). As with the Cp complexes, unusually low $\Delta S^{\ddagger}$ values are observed, again in accord with the proposed η^5-S → η^5-U reorganization (eq 17). Substitution of a methyl group in the 3-position of the pentadienyl ligand does not seem to bring about any significant effects, possibly since it is oriented away from the carbonyl ligand.

Addition of CO to 18-Electron Chromocenes. Under similar conditions (70 °C, [CO] = 5.6×10^{-3}] the rate of addition of CO is only slightly faster to $Cp(C_5H_7)CrCO$ ($k_{obsd} = 2.83 \times 10^{-5}$ s^{-1}) than $Cp^*(C_5H_7)CrCO$ ($k_{obsd} = 2.4 \times 10^{-5}$ s^{-1}). However, CO peaks attributable to formation of $Cp(\eta^3\text{-}2,4\text{-}C_7H_{11})Cr(CO)_2$ from $Cp(2,4\text{-}C_7H_{11})CrCO$ were not observed even after 12 h under these conditions, showing that its rate of addition of CO is much slower than those of the C_5H_7 systems. As postulated in the case of CO substitution, it again appears as if substituents on the Cp ring do not give rise to large steric effects. In contrast, the presence of two methyl groups on the pentadienyl ligand is sufficient to dramatically slow the rate of addition.

Addition of CO is 1 order of magnitude slower than the exchange reaction. The addition of CO involves an ultimate change in conformation of the pentadienyl ligand (S shaped to W shaped) and also necessitates a change in electronic configuration ($\eta^5 \rightarrow \eta^3$), in order that the dicarbonyl species avoids an unfavorable 20-electron count (Figure 5). Since the transition state must to some degree involve the change in coordination from $\eta^5 \rightarrow \eta^3$, it appears that this is a high-energy process (possibly reflected in the high $\Delta H^{\ddagger}$ of 19.5 kcal/mol) and provides evidence that no such bonding transformation (η^5 remains η^5) occurs in the CO exchange reactions (Figure 5).

Reactivity of 17-Electron vs 18-Electron Complexes. Previous studies showed that the rate of associative CO substitution of $V(CO)_6$ (17-electron) is 10^{10} times faster than for $Cr(CO)_6$ (18-electron) and can be contrasted with the relatively slow rates for half-open vanadocene and chromocene complexes.[4a] $Cp(C_5H_7)CrCO$ reacts at approximately the same rate ($k_1 = 4.23 \times 10^{-4}$ s^{-1}, 60 °C) as $Cp(C_5H_7)VCO$ ($k_1 = 2.73 \times 10^{-4}$ s^{-1}, 60 °C). This has been explained[4b] in terms of a lower activation energy for an associative substitution reaction of a 17-electron system compared to an 18-electron system and approximately similar activation energies for dissociative substitution involving 17-electron and 18-electron complexes. Therefore, differences in rates of dissociative ligand substitution of 17-electron and 18-electron systems may be smaller than for corresponding systems involving associative substitution.

Conclusions

These studies have demonstrated that the half-open chromocenes are quite different from chromocene and the open

chromocenes, particularly in having much shorter Cr-C(pentadienyl) bond distances than would otherwise be expected and in forming relatively strongly bound 18-electron ligand adducts. The formation of these adducts is additionally unusual in that a concomitant change in pentadienyl coordination from the usual η^5-U form to the unusual η^5-S form results. However, upon oxidation to the 17-electron cations, the pentadienyl ligand reverts back to the usual η^5-U form, demonstrating a narrow window of stability for the η^5-S coordination. Besides the 18-electron mono(ligand) adducts, it is also possible to prepare 18-electron bis(ligand) adducts, in which η^3-pentadienyl coordination is present.

Half-open chromocene carbonyl complexes undergo CO substitution via the same mechanism and at approximately the same rate as their 17-electron vanadium counterparts. Substituents on the pentadienyl ligand may cause steric acceleration of the rate of dissociation, while substituents on the cyclopentadienyl ligand appear to exert electronic influences that result in a retardation in rate. Unusually low, even negative, entropies of activation characterize these reactions and may be attributed to a reorganization of η^5-S to η^5-U pentadienyl coordination. The slow rates of CO addition to these complexes (which require an $\eta^5 \rightarrow \eta^3$ transformation of the pentadienyl ligand) suggest that no ring slippage occurs in the transition state of the CO substitution reactions.

Note Added in Proof. We have learned from Prof. Robert Waymouth of his group's recent syntheses and structural characterizations of $Cp^*(2,4\text{-}C_7H_{11})Cr$ and its monocarbonyl adduct. Both structures are consistent with those found in the present study.

Acknowledgment. F.B. and R.D.E. express their appreciation for generous support of this research by the National Science Foundation and a Faculty Fellow Award from the University of Utah (R.D.E.). We are grateful to R. M. Waymouth for providing details of his unpublished work.

Supplementary Material Available: Listings of IR and mass spectral data, anisotropic thermal parameters, hydrogen atom parameters, least-squares-plane data, positional parameters for non-hydrogen atoms, and bond distances and angles for $Cp(C_5H_7)Cr(CO)_2$ (19 pages); tables of observed and calculated structure factors (14 pages). Ordering information is given on any current masthead page.

Zinc and Magnesium Substitution in Hemoglobin: Cyclic Electron Transfer within Mixed-Metal Hybrids and Crystal Structure of MgHb

Debasish Kuila,[†] Michael J. Natan,[†] Paul Rogers,[‡] David J. Gingrich,[†] Wade W. Baxter,[†] Arthur Arnone,[‡] and Brian M. Hoffman*,[†]

Contribution from the Department of Chemistry, Northwestern University, 2145 Sheridan Road, Evanston, Illinois 60208, and Department of Biochemistry, University of Iowa, Iowa City, Iowa 52242. *Received December 24, 1990*

Abstract: Studies of long-range electron transfer within mixed-metal hemoglobin (Hb) hybrids [α_2(FeP), β_2(MP)] (M = Mg, Zn; P = protoporphyrin IX) are reported, along with the X-ray crystal structure of magnesium-substituted hemoglobin (MgHb). MgHb adopts the quaternary structure of deoxyHb, and replacement of Fe by Mg causes negligible structural changes, supporting earlier inferences that electron transfer (ET) in these hybrids occurs between redox centers held at fixed and crystallographically known distance and orientation. Upon flash photolysis of the [MP, $Fe^{3+}(H_2O)$P] hybrids, the charge-separated intermediate [$(MP)^+$, Fe^{2+}P] (I) is formed by a photoinitiated ^{3}(MP) $\rightarrow$ Fe^{3+}P intramolecular electron-transfer process with rate constant k_t and returns to the ground state by a $Fe^{2+}P \rightarrow (MP)^+$ thermal electron transfer with rate constant k_b. By use of the transient absorption technique, we have measured k_t and k_b for M = Mg and Zn as a function of temperature between 0 and 25 °C. The rate constant, k_t = 35 (8) s^{-1}, for Mg at room temperature is significantly lower than that of Zn, k_t = 85 (15) s^{-1}, although the driving force is greater in the former by about 100 mV. The charge recombination rate, k_b, within [Zn, Fe] is 350 (35) s^{-1} compared to that of 155 (15) s^{-1} for [Mg, Fe]. The inequality, $k_{b,t}^{Zn} \neq k_{b,t}^{Mg}$, rules out rate-limiting conformational "gating" for photoinitiated and thermally activated electron-transfer processes, and further indicates that in both cases ET is direct. Comparisons among the rate constants indicate that the electronic-coupling matrix element between redox sites, $|H_{AB}|^2$, may be slightly (roughly 2-fold) greater for M = Zn than for M = Mg.

Recently it has become possible to study long-range interprotein electron transfer[1] without the complication of second-order processes, through use of modified proteins that hold an electron donor/acceptor redox pair at a fixed distance.[2] In one approach, long-range electron transfer within protein-protein complexes can be accomplished by replacing the heme (FeP) of one protein partner with a closed-shell porphyrin MP[3] (M = Zn, Mg; P = protoporphyrin IX), which permits a photoinitiated ET cycle that begins with the ^{3}(MP) $\rightarrow$ Fe^{3+}P process.[4,5] Mixed-metal [MP, FeP] hemoglobin (Hb) hybrids are particularly suited to the study of long-range electron-transfer processes because replacement of Fe with these closed-shell metal ions causes negligible perturbation of the protein structure. For example, the X-ray crystal structure

[†] Northwestern University.
[‡] University of Iowa.

(1) (a) Gray, H. B.; Malmström, B. G. *Biochemistry* **1989**, *28*, 7499-7505. (b) Marcus, R. A.; Sutin, N. *Biochim. Biophys. Acta* **1985**, *811*, 265-322.

(2) (a) McLendon, G. *Acc. Chem. Res.* **1988**, *21*, 160-167. (b) Cowan, J. A.; Upmacis, R. K.; Beratan, D. N.; Onuchic, J. N.; Gray, H. B. *Ann. N.Y. Acad. Sci.* **1988**, *550*, 68-84. (c) Zang, L.-H.; Maki, A. H. *J. Am. Chem. Soc.* **1990**, *112*, 4346-4351. (d) Therien, M. J.; Selman, M.; Gray, H. B.; Chang, I.-Jy.; Winkler, J. R. *J. Am. Chem. Soc.* **1990**, *112*, 2420-2422. (e) Canters, G. W.; Hali, F. C.; Floris, R.; van de Kamp, M. *J. Am. Chem. Soc.* **1990**, *112*, 907-908.

(3) Abbreviations: hemoglobin, Hb; metalloprotoporphyrin IX, MP; metal-substituted hemoglobin, MHb; mixed-metal hemoglobin hybrids [MP, FeP]; high-performance liquid chromatography, HPLC; isoelectric focusing, IEF; potassium phosphate, KP_i; inositol hexaphosphate, IHP.

0002-7863/91/1513-6520$02.50/0